Optical and microwave control of resonance fluorescence and squeezing spectra in a polar molecule

M. A. Antón,[1] S. Maede-Razavi,[2] F. Carreño,[1,*] I. Thanopulos,[3] and E. Paspalakis[4]

[1]*Faculty of Optics and Optometry, University Complutense of Madrid, C/ Arcos de Jalón 118, 28037 Madrid, Spain*
[2]*Department of Physics, College of Science, University of Yasouj, Iran*
[3]*Department of Optics and Optometry, T.E.I. of Western Greece, 251 00 Aigio, Greece*
[4]*Materials Science Department, University of Patras, 265 04 Patras, Greece*

A two-level quantum emitter with broken inversion symmetry simultaneously driven by an optical field and a microwave field that couples to the permanent dipole's moment is presented. We focus to a situation where the angular frequency of the microwave field is chosen such that it closely matches the Rabi frequency of the optical field, the so-called Rabi resonance condition. Using a series of unitary transformations we obtain an effective Hamiltonian in the double-dressed basis which results in easily solvable Bloch equations which allow us to derive analytical expressions for the spectrum of the scattered photons. We analyze the steady-state population inversion of the system which shows a distinctive behavior at the Rabi resonance with regard to an ordinary two-level nonpolar system. We show that saturation can be produced even in the case that the optical field is far detuned from the transition frequency, and we demonstrate that this behavior can be controlled through the intensity and the angular frequency of the microwave field. The spectral properties of the scattered photons are analyzed and manifest the emergence of a series of Mollow-like triplets which may be spectrally broadened or narrowed for proper values of the amplitude and/or frequency of the low-frequency field. We also analyze the phase-dependent spectrum which reveals that a significant enhancement or suppression of the squeezing at certain sidebands can be produced. These quantum phenomena are illustrated in a recently synthesized molecular complex with high nonlinear optical response although they can also occur in other quantum systems with broken inversion symmetry.

I. INTRODUCTION

In the past four decades, resonance fluorescence has attracted great attention within the quantum optics community. Despite its conceptual simplicity, it entails a wide range of intriguing phenomena such as the Mollow-triplet emission spectrum [1] and photon antibunching [2,3]. Recently, renewed interest on this topic has emerged due to potential applications in quantum-information science [4] using systems such as trapped atoms or ions, as well as semiconductor quantum dots (QDs). As a matter of fact, quantum optical experiments pioneered in atomic vapors in the 1970s have been shown to be achievable in these systems [5–10]. Further developments addressed the problem to determine the atomic resonance fluorescence spectrum (RFS) under conditions of bichromatic excitation based upon the use of two driving fields with two slightly different angular frequencies which interact with the atom through the transition dipole moment [11,12]. Under such driving conditions a novel multiplet structure emerged in the RFS [13–15] and in the absorption spectrum [14]. The analysis of RFS in a two-level system has been recently extended to the case of a polychromatic excitation [16].

An important nonclassical feature of the resonance fluorescence spectrum is the squeezing of the field quadratures of a two-level system, which was theoretically addressed by Walls and Zoller [17] and later experimentally verified [18]. Due to its potential applications in high-precision measurements like gravitational wave detection [19], quantum teleportation [20],

and quantum computing [21], the squeezing of the fluorescent field has been widely studied in two- and three-level atoms driven by laser fields [22]. In connection with the development of quantum informatics, squeezed states of the radiation field have been recognized as crucial resources for continuous variable quantum information processing [23–25]. Therefore, the issue of generation of fields with enhanced squeezing is still an interesting topic. Squeezing in resonance fluorescence has been experimentally realized in QDs [26]. In the field of quantum plasmonics the squeezed spectrum of a single quantum emitter placed adjacent to a gold nanosphere [27,28] or a graphene sheet [29] has been analyzed.

All these theoretical and experimental studies have been developed in the framework of symmetric quantum emitters where inversion symmetry is assumed. However, the violation of the inversion symmetry is inherent in many quantum systems and results in nonzero permanent dipole matrix elements (PDMs) of the ground and excited states. For example, in polar molecules [30] the origin is the parity mixing of the molecular states, while in asymmetric QDs it arises due to the asymmetry of the confining potential of the dot. The existence of nonzero PDMs has been experimentally observed in several systems [31–37]. Furthermore, the presence of PDMs considerably influences the optical response of a system [38–40] leading, for example, to changes in multiphoton resonant excitation [41–43], modifications of the saturation of absorption and dispersion [44], creation of second-harmonic generation [45] and correlated photon pairs [46], as well as the opening of new optical transitions [47–49]. The bichromatic excitation of quantum systems with PDMs has been studied in a wide range of quantum systems, including electron and nuclear

_____
*ferpo@fis.ucm.es

spins [50,51], QDs [52,53], and superconducting qubits [54]. The RFS of an asymmetric QD has been recently analyzed in the regime of dissipative dynamics and weak frequency modulation of the low-frequency (LF) field [55,56].

In this paper we develop a theoretical description of the properties of the scattered field by a quantum emitter with broken inversion symmetry simultaneously driven by a transverse optical field and a longitudinal low-frequency (LF) field with angular frequencies ω_L and ω_s, respectively. We focus on a situation where the Rabi frequency Ω_R of the optical field is close to ω_s, i.e., $\omega_s \simeq \Omega_R$ holds, a situation which is termed as the Rabi resonance condition. In such circumstances the optical field couples to the transition dipole moment of the emitter, while the LF field couples the PDMs to the population inversion. This situation differs from those previously mentioned of bichromatic driving where the two fields have angular frequencies within the same range and both fields coupled to the transition dipole moment of the quantum transition [11–15]. We derive a master equation for the reduced density matrix by making use of a Furry-based unitary transformation approach which includes the interaction with PDMs nonperturbatively. By doing that we arrive at an effective Hamiltonian which differs from the one obtained in Ref. [24], which in turn manifests notable differences at steady state when obtained by the two methods. The effective Hamiltonian is obtained in the doubly dressed basis allowing one to derive analytical expressions for the resonance fluorescence and the squeezing spectra. We show that the RFS may exhibit up to nine spectral components grouped into three triplets, a result which contrasts to the Mollow triplet in nonpolar systems. The peak value of each spectral line is shown to depend on how close to the Rabi resonance condition the two driving fields are. In addition, the LF field is shown to be a knob to tune the spectral features. Moreover, squeezing of the scattered field in a wide spectral range is generated which can be controlled by the LF field and the phase of the local oscillator.

The paper is organized as follows. Section II establishes the model, i.e., the Hamiltonian of the system and the time-evolution equations of the quantum system operators taking into account the counter-rotating terms introduced by the PDMs. In order to arrive at a solvable master equation for the reduced density operator we introduce a general treatment based on unitary transformations and provide the key steps to derive the master equation for the reduced density matrix. The transformation to doubly dressed states of the quantum system in the strong-field limit allows us to obtain the analytical expressions for the spectra. Section III presents numerical simulations which illustrate the effect of the LF field on the spectra. Section IV summarizes the main findings of our work. Finally, two Appendixes are provided with details of intermediate calculations.

II. THEORETICAL MODEL

We consider a two-level system with ground (excited) state $|1\rangle$ ($|2\rangle$) and energy $\hbar\omega_1$ ($\hbar\omega_2$), as the one depicted in Fig. 1. The transition frequency is $\omega_0 = \omega_2 - \omega_1$, and the transition electric dipole moment is $\vec{\mu}_{12}$. Due to the breaking of inversion symmetry the levels $|1\rangle$ and $|2\rangle$ may exhibit unequal PDMs
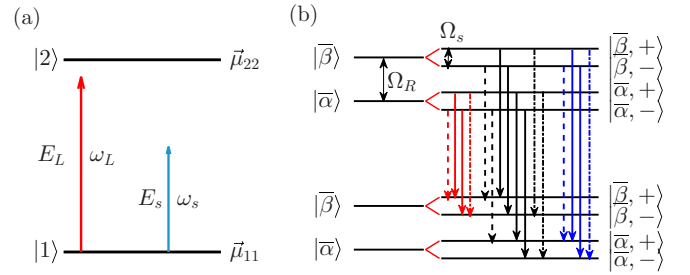
FIG. 1. (a) Energy-level diagram of the two-level system. The external field (E_L) of frequency ω_L drives the electronic transition and the LF field (E_s) with frequency $\omega_s \ll \omega_L$ modulates the resonance frequency. The two-level scheme illustrates the molecule with permanent electric dipole moments in the ground and excited states $\vec{\mu}_{11}$, and $\vec{\mu}_{22}$, respectively. (b) Dressed states of the bichromatically driven two-level polar system accounting for the red detuned, the central, and the blue detuned triplets. Vertical solid lines account for transitions contributing to the central line of each triplet, while vertical dashed (dashed-dotted) lines indicate the transitions which produce the red(blue) detuned line within each triplet.

($\vec{\mu}_{11} \neq \vec{\mu}_{22}$). The optical transition $|1\rangle \leftrightarrow |2\rangle$ is driven by a linearly polarized laser field of frequency ω_L given by

$$\hat{E}_L(t) = \tfrac{1}{2} E_L (e^{-i\omega_L t} + e^{i\omega_L t}) \hat{u}, \qquad (1)$$

where E_L is the electric-field amplitude and $\hat{u}$ the unit polarization vector. We assume that $\hat{u} \| \vec{\mu}_{12} \| \vec{\mu}_{11} \| \vec{\mu}_{22}$. The quantum system is also driven by a monochromatic LF field of amplitude E_s and angular frequency $\omega_s \ll \omega_L$ given by

$$\hat{E}_s(t) = \tfrac{1}{2} E_s (e^{-i\omega_s t} + e^{i\omega_s t}) \hat{u}. \qquad (2)$$

The Hamiltonian of the system can be expressed as

$$H = H_0^M + H_0^B + H_{B-M} + H_{\text{drive}}, \qquad (3)$$

where

$$H_0^M = \hbar \frac{\omega_0}{2} \hat{\sigma}_z,$$

$$H_0^B = \hbar \sum_k \omega_k a_k^\dagger a_k, \qquad (4)$$

$$H_{B-M} = \hbar \sum_k g_k (a_k^\dagger + a_k)(\hat{\sigma}^+ + \hat{\sigma}^-).$$

The first term H_0^M describes a two-level system with a transition frequency ω_0, and $\hat{\sigma}^\pm$, $\hat{\sigma}_z$ are the Pauli matrices acting in the space spanned by the states $|1\rangle$ and $|2\rangle$. The second term H_0^B corresponds to the free energy of the environmental electromagnetic vacuum modes, where a_k ($a_k^\dagger$) is the annihilation (creation) operator of the kth mode of the vacuum field with polarization $\vec{e}_k$ and angular frequency ω_k. The third term represents the interaction between the quantum system and the vacuum modes. The parameter g_k is the coupling constant of the electronic transition $|2\rangle \rightarrow |1\rangle$ with the electromagnetic vacuum mode $g_k = \sqrt{\frac{\omega_k}{2\hbar\epsilon_0 V}} (\vec{\mu}_{12} \cdot \hat{e}_k)$, $\hat{e}_k$ being the unit vector of the radiation mode and V the quantization volume. Finally, the Hamiltonian H_{drive} describes the interaction of the quantum system with the external electromagnetic field and can be

constructed as follows. The interaction of a classical dipole **d** with an external electric field $\mathcal{E}$ is given by the expression $H_{\text{drive}} = \mathbf{d} \cdot \mathcal{E}$, and within the quantum-field approach we have to replace the classical dipole **d** with the corresponding operator

$$\mathbf{d} = \frac{\vec{\mu}_{22} + \vec{\mu}_{11}}{2}\hat{I} + \frac{\vec{\mu}_{22} - \vec{\mu}_{11}}{2}\hat{\sigma}_z + \vec{\mu}_{21}\hat{\sigma}^+ + \vec{\mu}_{12}\hat{\sigma}^-, \quad (5)$$

where $\hat{I}$ is the identity operator. Thus the interaction Hamiltonian can be written as

$$\begin{aligned} H_{\text{drive}} = {} & \hbar\Omega(e^{-i\omega_L t} + e^{i\omega_L t})(\hat{\sigma}^+ + \hat{\sigma}^-) \\ & + \hbar G(e^{-i\omega_s t} + e^{i\omega_s t})(\hat{\sigma}^+ + \hat{\sigma}^-) \\ & + \hbar\frac{\Omega}{2}(e^{-i\omega_L t} + e^{i\omega_L t})\hat{\sigma}_z \\ & + \hbar\frac{G}{2}(e^{-i\omega_s t} + e^{i\omega_s t})\hat{\sigma}_z, \end{aligned} \quad (6)$$

$\Omega \equiv \frac{\mu_{12}E_L}{2\hbar}$ being the Rabi frequency of the laser field and $G \equiv \frac{\mu_0 E_s}{2\hbar}$ standing for the Rabi frequency of the LF field. In these expressions, $\mu_0 = |\vec{\mu}_{22} - \vec{\mu}_{11}|$, and we have assumed $\vec{\mu}_{12} = \vec{\mu}_{21}$ (real).

Our aim is to obtain the time evolution of the density matrix. To do that we apply a method based on a series of unitary transformations in order to eliminate the explicit temporal dependence introduced by the LF field in the diagonal elements of the Hamiltonian of Eq. (6). The first unitary transformation allows one to remove the fast oscillating terms in Eq. (6) by moving to a frame rotating at ω_L and is given by

$$U_1 = e^{-i(\frac{1}{2}\omega_L\hat{\sigma}_z + \sum_k \omega_k a_k^\dagger a_k)t}. \quad (7)$$

In the new frame the density matrix is given by $\rho^{(1)} = U_1^\dagger(t)\rho^{(s)}(t)U_1(t)$ and the resulting Hamiltonian is $H^{(1)}(t) = U_1^\dagger(t)H(t)U_1(t) - i\hbar U_1^\dagger(t)\frac{\partial U_1(t)}{\partial t}$, yielding

$$\begin{aligned} H^{(1)} = {} & \hbar\frac{\Delta_L}{2}\hat{\sigma}_z + \hbar\Omega(\hat{\sigma}^+ + \hat{\sigma}^-) \\ & + \hbar G(\hat{\sigma}^+ e^{-i(\omega_s - \omega_L)t} + \hat{\sigma}^- e^{+i(\omega_s - \omega_L)t}) \\ & + \hbar\frac{\Omega}{2}(e^{-i\omega_L t} + e^{i\omega_L t})\hat{\sigma}_z + \hbar\frac{G}{2}(e^{-i\omega_s t} + e^{i\omega_s t})\hat{\sigma}_z \\ & + \hbar\sum_k g_k(a_k^\dagger\hat{\sigma}^- e^{i(\omega_k - \omega_L)t} + \hat{\sigma}^+ a_k e^{-i(\omega_k - \omega_L)t}), \quad (8) \end{aligned}$$

where $\Delta_L = \omega_0 - \omega_L$ is the detuning of the optical field with the transition frequency.

At this point it is worth noting the difference between the Hamiltonian in Eq. (8) and the Hamiltonian considered in previous works [11–14]. Note that in writing Eq. (8) the rotating wave approximation for the optical field has been assumed. In all those previous cases the pump and probe fields had similar angular frequencies that were tuned close to the transition frequency (ω_0), and more importantly, both fields interact with the quantum system via transition dipole moment. To illustrate this point, let us consider the term oscillating at $\omega_s - \omega_L$ in Eq. (8). A term similar to this (although changing G to Ω') is the one that was considered in previous works concerning bichromatic driving [11–14] and when both ω_s and ω_L are within the same spectral range this term must be kept. However, in the situation addressed in this work the angular frequency of the LF field (ω_s) is more than six orders of magnitude lower than the transition frequency (ω_0), whereas the optical field (ω_L) drives the transition dipole close to resonance. Thus the interaction of the LF field with the transition dipole moment averages to zero. In a similar way, the interaction of the optical field with the PDMs (the term oscillating at ω_L) averages to zero, whereas the interaction of the LF field with the PDMs of the system (the term oscillating at ω_s) must be retained. In addition, when assuming that ω_s is a low frequency we are allowed to reach a physical situation in which such frequency is tuned close to the Rabi frequency of the optical pump field. Such Rabi resonance condition is far from being reached in the case were the two fields are within the optical range. Thus the following conditions hold: (i) $\Omega \gg G$ and (ii) $\Omega - \omega_s \ll \omega_s$. In view of the previous considerations we get the same Hamiltonian as the one considered in Ref. [57], although in what follows we perform a series of unitary transformations some of them being time dependent in order to obtain an effective Hamiltonian.

In the current case the strong driving field E_L can be viewed as a dressing field for the two-level system. Under these conditions we resort to diagonalizing the quantum system part of the Hamiltonian and the interaction of the quantum system with the laser field

$$H^{(01)} = \hbar\frac{\Delta_L}{2}\hat{\sigma}_z + \hbar\Omega(\hat{\sigma}^+ + \hat{\sigma}^-), \quad (9)$$

by means of a canonical transformation $U_2 = e^{-i\theta\sigma_y}$, with $\sin(2\theta) = \frac{\Delta_L}{\Omega_R}$, $\cos(2\theta) = \frac{2\Omega}{\Omega_R}$, and $\Omega_R \equiv \sqrt{\Delta_L^2 + (2\Omega)^2}$. With these relations in mind, the Hamiltonian $H^{(1)}$ in Eq. (8) becomes

$$\begin{aligned} H^{(2)} = {} & \hbar\frac{\Omega_R}{2}R_z + \hbar\frac{G}{2}(e^{-i\omega_s t} + e^{i\omega_s t})\big[(c_1^2 - s_1^2)R_z - 2c_1 s_1(R^+ + R^-)\big] \\ & + \hbar\sum_k g_k\big[a_k^\dagger e^{i(\omega_k - \omega_L)t}(c_1 s_1 R_z + c_1^2 R^- - s_1^2 R^+) + \text{H.a.}\big], \quad (10) \end{aligned}$$

where $c_1 = \cos(\theta)$ and $s_1 = \sin(\theta)$, and H.a. stands for Hermitian adjoint. The operators R^+, R^+, and R_z appearing in Eq. (10) refer to the eigenstates of $H^{(01)}$ given in Appendix A.

The next step to eliminate the explicit time dependence in Eq. (10) relies on the use of the Furry representation [58]. To this end we make use of the unitary transformation defined as

$$U_3(t) = e^{-i[\frac{\Omega_R}{2}t + \frac{2G\cos(2\theta)}{\omega_s}\sin(\omega_s t)]R_z}. \quad (11)$$

The resulting Hamiltonian is given by

$$H^{(3)} = -\hbar G c_1 s_1 \left\{ \sum_l J_l(z)[R^+ e^{i[\Omega_R + (l-1)\omega_s]t} + R^- e^{-i[\Omega_R + (l-1)\omega_s]t}] + \sum_l J_l(z)[R^+ e^{i[\Omega_R + (l+1)\omega_s]t} + R^- e^{-i[\Omega_R + (l+1)\omega_s]t}] \right\}$$
$$+ \hbar U_3^\dagger(t) \sum_k g_k \left[a_k^\dagger e^{i(\omega_k - \omega_L)t} (c_1 s_1 R_z + c_1^2 R^- - s_1^2 R^+) + \text{H.a.} \right] U_3(t). \tag{12}$$

In arriving at Eq. (12) we made use of the Jacoby-Auger identity $\exp(iz \sin \omega_s t) = \sum_{n=-\infty}^{\infty} J_n(z) e^{n\omega_s t}$, with $J_n(z)$ being the Bessel function of the first kind of order n [59], and $z \equiv \frac{4G \cos(2\theta)}{\omega_s}$. Then, we assume the resonance condition: $\Delta_q \equiv \Omega_R - q\omega_s \ll \omega_s$, with q being an integer. After we apply the unitary transformation $U_4 = e^{i\frac{\Delta_s}{2} t R_z}$ (see Appendix A for details) we remove the oscillating terms in the coherent part of the Hamiltonian. Finally, since we are interested in the physics in the strong-driving regime, we move to the double-dressed picture in order to obtain analytical results. To do this we can diagonalize the resulting Hamiltonian $H^{(4)}$ in Eq. (A5) by means of a rotation operator $U_5 = e^{-i\phi\sigma_y}$ where $\sin(2\phi) = -\frac{\Delta_q}{\Omega_S}$, $\cos(2\phi) = \frac{2\Omega_R}{\Omega_S}$, and $\Omega_S \equiv \sqrt{\Delta_q^2 + (2\Omega_R)^2}$. The transformed matrix density $\rho^{(5)}(t)$ is given by

$$\frac{\partial \rho^{(5)}(t)}{\partial t} = -i\frac{\Omega_S}{2} [S_z, \rho^{(5)}] + L\rho^{(5)}, \tag{13}$$

where S_z, S_+, and S_-, are the system operators in the double-dressed basis and Ω_S is the frequency of the Rabi oscillations between the quantum states dressed simultaneously by the optical and LF fields. In the double-dressed basis the Liouvillian takes the form

$$L\rho^{(5)} = -\frac{\Gamma_0}{2} [S_z S_z \rho - S_z \rho S_z + \text{H.a.}]$$
$$- \frac{\Gamma_+}{2} [S^+ S^- \rho - S^- \rho S^+ + \text{H.a.}]$$
$$- \frac{\Gamma_-}{2} [S^- S^+ \rho - S^+ \rho S^- + \text{H.a.}], \tag{14}$$

and it describes the dynamics between the new dressed states $|+\rangle$ and $|-\rangle$ of the system. The parameters Γ_0, $\Gamma_\pm$ are given by

$$\Gamma_0 = \gamma_+ \sin^2(2\phi)/4 + \gamma_- \sin^2(2\phi)/4 + \gamma_0 \cos^2(2\phi),$$
$$\Gamma_+ = \gamma_+ \cos^4(\phi) + \gamma_- \sin^4(\phi) + \gamma_0 \sin^2(2\phi), \tag{15}$$
$$\Gamma_- = \gamma_+ \sin^4(\phi) + \gamma_- \cos^4(\phi) + \gamma_0 \sin^2(2\phi),$$

where γ_+, γ_-, and γ_o are given in Appendix A. These quantities determine the damping rates between the doubly dressed states of the system. In deriving Eq. (14) we only kept those terms which maintain the Linblad form, i.e., terms containing products of spin operator pairs $S^\pm$ with S_z, S^+ with S^+, and S^- with S^- were neglected. A similar approach was used in Ref. [57] [see their Eq. (12)].

In view of Eqs. (13) and (14), the Bloch equations in the double-dressed basis take the simple form

$$\frac{\partial \langle S^+(t)\rangle}{\partial t} = -[\Gamma_S - i\Omega_s]\langle S^+(t)\rangle,$$

$$\frac{\partial \langle S^-(t)\rangle}{\partial t} = -[\Gamma_S + i\Omega_s]\langle S^-(t)\rangle,$$
$$\frac{\partial \langle S_z(t)\rangle}{\partial t} = -\gamma_2 \langle S_z(t)\rangle + \gamma_{s0}, \tag{16}$$

where $\Gamma_S = 2\Gamma_0 + \gamma_2/2$, $\gamma_{s0} = \Gamma_- - \Gamma_+$, and $\gamma_2 = \Gamma_+ + \Gamma_-$. It becomes evident from Eq. (16) that we have to deal with easily solvable equations of motion and determining the initial conditions $\langle S^+(0)\rangle$, $\langle S^-(0)\rangle$, and $\langle S_z(0)\rangle$ is the only remaining problem. This task requires establishing the initial condition in the bare basis and transforming it to the double-dressed basis by making the unitary transformations used to arrive at Eq. (13). To this end we assume that in the bare basis $\rho(0) = \frac{1}{2} - \frac{1}{2}\rho_D(0)$ and $\rho_D(0) = -1$, i.e., the quantum system is initially in the ground state and there is no initial coherence. In view of that we get

$$\rho^{(5)}(0) = U^\dagger(0)\rho(0)U(0)$$
$$= U_5^\dagger U_2^\dagger(t)\rho(0)U_2 U_5$$
$$= \frac{1}{2} + \frac{1}{2}\rho_D^{(0)}(0)[\cos(2\theta)\cos(2\phi)$$
$$- \sin(2\theta)\sin(2\phi)]\langle S_z(0)\rangle$$
$$- \frac{1}{2}\rho_D^{(0)}(0)[\cos(2\theta)\sin(2\phi)$$
$$+ \sin(2\theta)\cos(2\phi)][\langle S^+(0)\rangle + \langle S^-(0)\rangle]. \tag{17}$$

The integration of Eqs. (16) yields a simple analytical solution

$$\langle S^+(t)\rangle = (\langle S^-(t)\rangle)^*$$
$$= \frac{\cos(2\theta)\sin(2\phi) + \sin(2\theta)\cos(2\phi)}{2} e^{-(\Gamma_S - i\Omega_s)t},$$
$$\langle S_z(t)\rangle = \frac{\gamma_{s0}}{\gamma_2}(1 - e^{-\gamma_2 \tau}) - [\cos(2\theta)\cos(2\phi)$$
$$- \sin(2\theta)\sin(2\phi)]e^{-\gamma_2 t}. \tag{18}$$

III. NUMERICAL RESULTS AND DISCUSSION

In order to illustrate the influence of PDMs on the optical response of a polar two-level system we use parameters suitable for a zinc-phthalocyanine molecular complex shown in Fig. 2, which has been recently synthesized and has shown large nonlinear optical response [60]; the parameters are obtained by *ab initio* electronic structure methods [61]. In our calculations, the ground electronic state and the first singlet electronic state of this complex are the states $|1\rangle$ and $|2\rangle$ according to our theoretical model, respectively. The spectroscopic parameters needed in the calculations are obtained after geometry optimization of the molecular structure of state $|1\rangle$ at the DFT/B3LYP/6-311+G* level of theory [61], while for state $|2\rangle$ the geometry optimization of the molecular structure
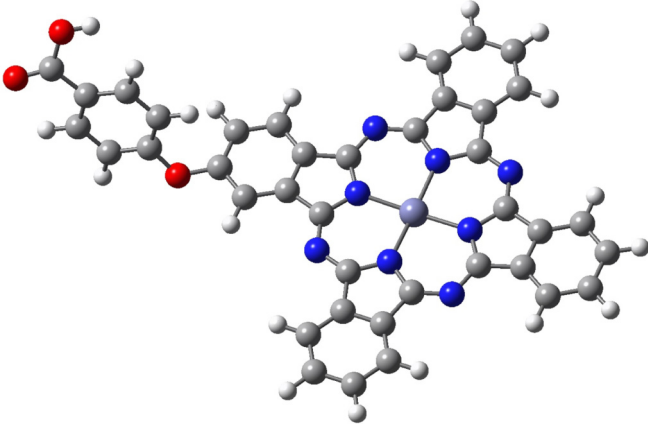
FIG. 2. Zinc-phthalocyanine complex used as a prototype polar molecule in this paper. The complex is composed of carbon (gray), hydrogen (white), oxygen (red), nitrogen (blue), and zinc (light blue) atoms.

was obtained at the TD-DFT/B3LYP/6-31-G* level of theory [61]. It is worth mentioning that the analysis presented in this work is not restricted to the specific quantum system but can be applied to various quantum systems with broken inversion symmetry.

From these calculations we obtain that the transition frequency is $\hbar\omega_0 = 1.99$ eV, the value of the transition electric dipole moment is $\mu_{12} = -3.25$ D, and the PDMs are $\mu_{11} = 7.27$ D and $\mu_{22} = 6.71$ D. The free-space radiative decay rate associated to the transition is about $\gamma \approx 13.6$ MHz. The intensity of the optical field is in the order of

$I_0 = 9.4 \times 10^3$ W/m^2, and typical values for the angular frequency of the LF field are around $\omega_s = 40\gamma \approx 540$ MHz, i.e., they are in the microwave region. These values are accessible with current experimental capabilities.

A. Steady-state population inversion

As a first step of our study we consider the effect of PDMs on the steady-state population of the system. This study will reveal the appearance of an unusual behavior near the Rabi resonance condition. This will help us to select the point of operation (detuning of the optical field) to analyze the spectral properties of the scattered field.

In order to analyze the dynamics of the population inversion it is convenient to express the physical quantities in terms of the density-matrix elements in the doubly dressed basis. We consider the inversion to be given as

$$\langle \sigma_z(t) \rangle = \text{Tr}[\sigma_z \rho(t)]. \tag{19}$$

Note that the density matrix $\rho(t)$ in Eq. (19) is related to $\rho^{(5)}(t)$ through the transformation $\rho^{(5)}(t) = U^\dagger(t)\rho(t)U(t)$, where $U(t) = U_1(t)U_2(t)U_3(t)U_4(t)U_5(t)$. Thus Eq. (19) can be rewritten in terms of $\rho^{(5)}$ as

$$\langle \sigma_z(t) \rangle = \text{Tr}\,[\sigma_z \rho(t)]$$
$$= \text{Tr}\,[\sigma_z U(t)\rho^{(5)}(t)U^\dagger(t)]$$
$$= \text{Tr}\,[U^\dagger(t)\sigma_z U(t)\rho^{(5)}(t)]. \tag{20}$$

After a series of straightforward calculations, Eq. (20) is given in terms of $S^\pm$ and S_z operators with time-dependent coefficients,

$$\langle \sigma_z(t) \rangle = \langle S_z(t) \rangle \left[\cos 2(\theta)\cos(2\phi) - \sin(2\theta)\sin(2\phi)\frac{e^{i\alpha(t)} + e^{-i\alpha(t)}}{2} \right]$$
$$- \langle S^+(t) \rangle \left[\cos(2\theta)\sin(2\phi) + \frac{e^{i\alpha(t)}}{2}[\sin(2\theta)\cos(2\phi) + \sin(2\theta)] + \frac{e^{-i\alpha(t)}}{2}[\sin(2\theta)\cos(2\phi) - \sin(2\theta)] \right]$$
$$- \langle S^-(t) \rangle \left[\cos(2\theta)\sin(2\phi) + \frac{e^{i\alpha(t)}}{2}[\sin(2\theta)\cos(2\phi) - \sin(2\theta)] + \frac{e^{-i\alpha(t)}}{2}[\sin(2\theta)\cos(2\phi) + \sin(2\theta)] \right], \tag{21}$$

where we have defined

$$e^{i\alpha(t)} = e^{i[q\omega_s t + z\,\sin(\omega_s t)]} = \sum_n J_n(z)e^{i(n+q)\omega_s t} \equiv Y_{nq}(t). \tag{22}$$

Note that after Eq. (18) we have that $\langle S^+(\infty) \rangle = \langle S^-(\infty) \rangle = 0$ and $\langle S_z(\infty) \rangle = \gamma_{s0}/\gamma_2$; thus the steady-state inversion in the bare basis can be expressed as

$$\langle \sigma_z(\infty) \rangle = \frac{\gamma_{s0}}{\gamma_2}[\cos(2\theta)\cos(2\phi) - \sin(2\theta)\sin(2\phi)J_{-q}(z)]. \tag{23}$$

It is worth noting that the result obtained in Eq. (23) reduces to the one obtained in Ref. [57] by setting $J_{-q}(z)$ equal to unity. This difference arises from the different approaches followed in Ref. [57] and in this work.

It is well known that in a nonpolar two-level system the steady-state inversion exhibits a Lorentzian shape with a

maximum at resonance [as shown with the dashed curve in Figs. 3(a) and 3(b)]. The effect of the LF on the steady-state population inversion in the bare basis as a function of the laser detuning Δ_L is shown in Fig. 3(a). There we observe that in the weak excitation regime (solid curve) two symmetric ultranarrow peaks appear superimposed over a broad Lorentzian line. This behavior is a distinctive feature of the polar character of the system driven by the LF field. The spectral location of these two peaks is obtained where the Rabi resonance condition $\Delta_{q=1} = 0$ is met. The linewidth of these narrow peaks increases as the value of G becomes larger, as it is shown with the dashed-dotted and dotted curves. This power broadening is better appreciated by looking at panel (b) where a zoom of the left Rabi resonance shown in panel (a) is depicted. The peaks have their origin in the existence of the pumping term $\hbar G \sin(2\theta)(-1)^{q+1}\frac{2q J_q(z)}{z}$ in Eq. (A5). We finally show in Fig. 3(c) how the change of the angular
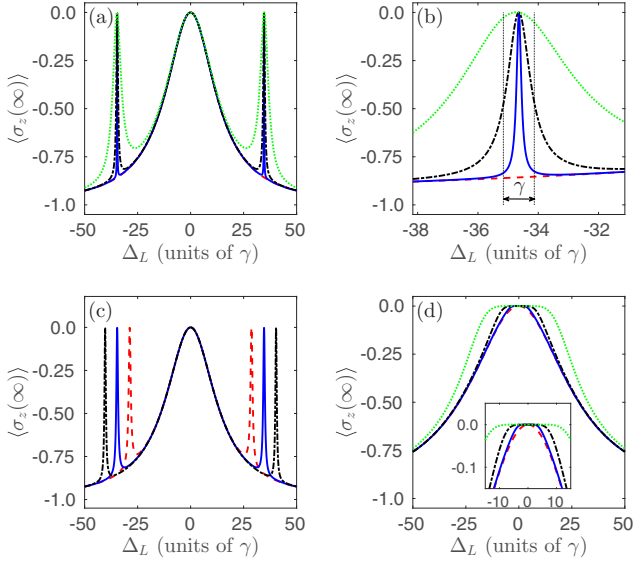
FIG. 3. (a) Steady state of the population inversion in the bare basis vs the detuning of the optical field Δ_L for different values of the Rabi frequency of the auxiliary field G: $G = 0$ (dashed curve), $G = 0.1\gamma$ (solid curve), $G = 0.5\gamma$ (dashed-dotted curve), and $G = 2.5\gamma$ (dotted curve). Other parameters: $\omega_s = 40\gamma$, $q = 1$, and $\Omega = 10\gamma$. (b) Zoom of panel (a) around the left Rabi resonance. (c) Steady state of the population inversion in the bare basis vs the detuning of the optical field Δ_L for different values of the angular frequency of the LF field: $\omega_s = 35\gamma$ (dashed curve), $\omega_s = 40\gamma$ (solid curve), and $\omega_s = 45\gamma$ (dashed-dotted curve). Other parameters used are $G = 0.5\gamma$ and the rest of the parameters as in panel (a). (d) Steady state of the population inversion in the bare basis vs the detuning of the optical field Δ_L for different values of the Rabi frequency of the auxiliary field G: $G = 0$ (dashed curve), $G = 0.1\gamma$ (solid curve), $G = 0.5\gamma$ (dashed-dotted curve), and $G = 2.5\gamma$ (dotted curve). Other parameters: $\omega_s = 40\gamma$, $q = 1$, and $\Omega = 20\gamma$.

frequency ω_s of the LF field can be used to tune the spectral location of the Rabi resonance.

Up to now we have considered a situation where Rabi resonance is obtained at $\Delta_L \neq 0$. However, the Rabi resonance condition ($\Delta_{q=1} = 0$) can be also achieved when driving the system on resonance; let us consider the case with $\Delta_L = 0$, which in turn requires the increase of the Rabi frequency Ω while $\Delta_{q=1} = 0$ still holds. In the current situation this happens when $\Omega = 20\gamma$. Here, the influence of PDMs on population inversion manifests itself in the emergence of a broad range of frequencies where saturation takes place, as it is shown in Fig. 3(d).

B. Resonance fluorescence spectrum

In view of the previous results, the control of the Rabi resonance condition could be used as a knob for tailoring the spectral properties of the scattered photons. As a first step we consider the RFS. It is well known that the RFS can be written as a sum of two parts [62],

$$S(\omega) = S_{\text{coh}}(\omega) + S_0(\omega), \tag{24}$$

where $S_{\text{coh}}(\omega)$ stands for the coherent (elastic) part of the spectrum, and

$$S_0(\omega) = 2\,\text{Re}\left[\lim_{t \to \infty} \int_0^\infty \langle \delta\sigma^+(t+\tau) \cdot \delta\sigma^-(t)\rangle e^{-i\omega\tau} d\tau\right] \tag{25}$$

is the incoherent (noise) part of the spectrum. Here, $\delta\sigma^+(t) = \sigma^+(t) - \langle\sigma^+(t)\rangle$ stands for the deviation of the dipole polarization operator from its mean steady-state value and Re denotes the real part. For the fluorescence spectrum, it is sufficient to evaluate the integral (25) in the steady-state limit. In this limit, due to the time-dependent unitary transformations $U_j(t)$, the correlation function can be expressed as

$$\langle\delta\sigma^+(t+\tau) \cdot \delta\sigma^-(t)\rangle = \text{Tr}\left[U^+(t)\delta\sigma^+(t)U(t)e^{-i\frac{H^{(5)}}{\hbar}\tau}U^+(t)\delta\sigma^-(t)U(t)\rho^{(5)}(t)e^{i\frac{H^{(5)}}{\hbar}\tau}\right]$$

$$= \text{Tr}\left[e^{i\frac{H^{(5)}}{\hbar}\tau}U^+(t)\delta\sigma^+(t)U(t)e^{-i\frac{H^{(5)}}{\hbar}\tau}U^+(t)\delta\sigma^-(t)U(t)\rho^{(5)}(t)\right]. \tag{26}$$

The transform $U^+(t)\sigma^\pm(t)U(t)$ in the correlation function can be expressed in terms of $\delta S^\pm$ and δS_z with time-dependent coefficients (see Appendix B) and results in

$$U^+(t)\delta\sigma^\pm(t)U(t) = f_0\left[Y_{nq}(t)\frac{\cos 2\theta \pm 1}{2}\sin 2\phi + Y_{nq}^*(t)\frac{\cos 2\theta \mp 1}{2}\sin 2\phi + \sin 2\theta\,\cos 2\phi\right]\delta S_z(t)$$

$$+ f_0\left[Y_{nq}(t)\frac{(\cos 2\theta \pm 1)(\cos 2\phi + 1)}{2} + Y_{nq}^*(t)\frac{(\cos 2\theta \mp 1)(\cos 2\phi - 1)}{2} - \sin 2\theta\,\sin 2\phi\right]\delta S^+(t)$$

$$+ f_0\left[Y_{nq}(t)\frac{(\cos 2\theta \pm 1)(\cos 2\phi - 1)}{2} + Y_{nq}^*(t)\frac{(\cos 2\theta \mp 1)(\cos 2\phi + 1)}{2} - \sin 2\theta\,\sin 2\phi\right]\delta S^-(t), \tag{27}$$

where $f_0 = \frac{e^{\pm i\omega_L t}}{2}$.

Starting from Eqs. (25)–(27), invoking the quantum regression theorem [63] and using the fact that $\langle\delta S^-(\infty)\rangle = \langle\delta S^+(\infty)\rangle = 0$, we reach an analytical expression for the RSF (see Appendix B), namely

$$S_0(\omega) = S_{(zz)}(\omega) + S_{(+-)}(\omega) + S_{(-+)}(\omega), \tag{28}$$

where

$$S_{(zz)}(\omega) = \frac{1 - \langle S_z(\infty) \rangle^2}{4} \left[\sum_n \frac{A_1 \gamma_2}{\gamma_2^2 + [\omega - \omega_L - (q+n)\omega_s]^2} + \sum_n \frac{A_2 \gamma_2}{\gamma_2^2 + [\omega - \omega_L + (q+n)\omega_s]^2} + \frac{A_3 \gamma_2}{\gamma_2^2 + (\omega - \omega_L)^2} \right], \quad (29)$$

$$S_{(+-)}(\omega) = \frac{1 + \langle S_z(\infty) \rangle}{8} \left[\sum_n \frac{B_1 \Gamma_s}{\Gamma_s^2 + [\omega - \omega_L - (q+n)\omega_s - \Omega_s]^2} \right.$$

$$\left. + \sum_n \frac{B_2 \Gamma_s^2}{\Gamma_s^2 + [\omega - \omega_L + (q+n)\omega_s - \Omega_s]^2} + \frac{B_3 \Gamma_s}{\Gamma_s + (\omega - \omega_L - \Omega_s)^2} \right], \quad (30)$$

$$S_{(-+)}(\omega) = \frac{1 - \langle S_z(\infty) \rangle}{8} \left[\sum_n \frac{C_1 \Gamma_s}{\Gamma_s^2 + [\omega - \omega_L - (q+n)\omega_s + \Omega_s]^2} \right.$$

$$\left. + \sum_n \frac{C_2 \Gamma_s}{\Gamma_s^2 + [\omega - \omega_L + (q+n)\omega_s + \Omega_s]^2} + \frac{C_3 \Gamma_s}{\Gamma_s^2 + (\omega - \omega_L + \Omega_s)^2} \right], \quad (31)$$

where expressions for the coefficients A_j, B_j, and C_j are provided in Appendix B.

The interaction of the strong field and the quantum system creates the dressed states, with energy splitting equal to Ω_R as shown in Fig. 1(b). In addition, the LF field with frequency ω_s, which is close to the effective Rabi frequency Ω_R, dresses the quantum system giving rise to a series of new doublets with energy splitting Ω_s. The allowed transitions between the doubly dressed states produce a series of triplets in the laboratory frame with amplitudes proportional to $\gamma_2 A_j$, $\Gamma_s B_j$, and $\Gamma_s C_j$ ($j = 1,2,3$) as indicated in Eqs. (29)–(31). The transitions from adjacent manifolds of dressed states indicated in Fig. 1(b) give rise to such series of triplets. We note that Eqs. (29)–(31) show that the positions, the widths, and the intensities of the nine peaks of the spectrum are all associated with the decay rate γ_2 and Γ_s which depend on the LF field parameters and the Rabi resonance condition.

We proceed to analyze the role of the interaction between the LF field and the PDMs on the RFS. Using the numerically calculated formal spectrum $S_0(\omega)$, given in Eqs. (28)–(31) we can now illustrate new spectral features caused by the presence of permanent dipole moments coupled to the LF field. In what follows we restrict ourselves to showing the RFS for the case with $q = 1$ and $n = 0$.

We start by considering the strong driving regime in the case that the optical field is at exact resonance with the transition frequency ($\Delta_L = 0$), $\Omega = 20\gamma$, and the angular frequency of the LF field is $\omega_s = 40\gamma$. Under this condition we achieve the Rabi resonance condition $\Delta_q = 0$. This situation corresponds to the case studied in Fig. 3(d). The spectra obtained for different values of the coupling with PDMs (G) are shown in Figs. 4(a)–4(c). Note that for the case of $G = 0$ we recover the Mollow triplet consisting of a central line around $\omega = 0$ and two outer sidebands located at $\pm 2\Omega_R$. However, when the LF is present the central line starts to split into two lines and the outer sidebands begin to broaden but their structure is unresolved as shown in panel 4(b). A further increase of G [panel 4(c)] results in the full development of the outer sidebands into spectrally resolved triplets while the central line develops into a doublet and the cancellation of the central

component at $\omega = 0$. This behavior clearly departs from the one of the nonpolar case shown in Fig. 4(a). The three terms contributing to the RFS in Eq. (28) are shown for the case with $G = 2.5\gamma$ in panel 4(d) where the central line is absent [the term proportional to A_3 in Eq. (29)] and two peaks centered at $\omega = \pm \Omega_s$ together with a blue detuned triplet and a red detuned triplet appear. The spectral lines corresponding to the centers of the triplets are given by the terms proportional to A_1 and A_2 in Eq. (29), whereas the spectral separation between the two peaks of the blue or red detuned triplet is $2\Omega_s$. For low values of the parameter G the triplets collapse into a single line and the two central peaks into a single line, as it can be observed for the limiting case shown in Fig. 4(a). It is worth noting that the spectral components of the scattered field display a symmetric
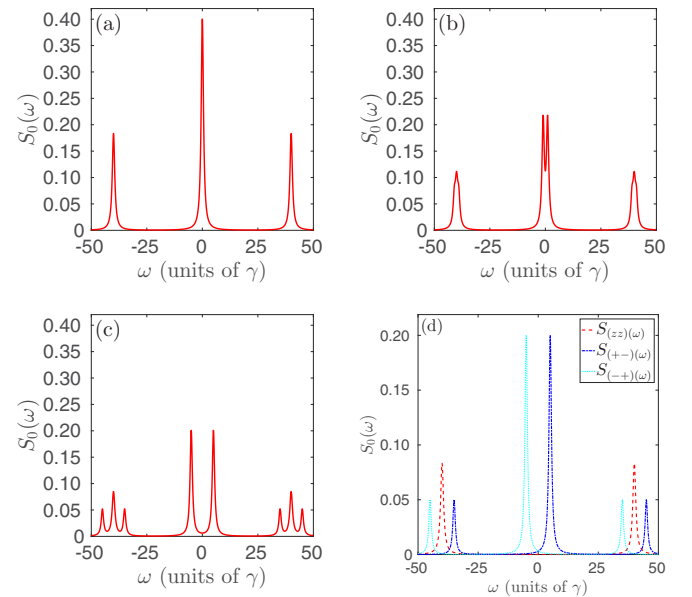
FIG. 4. RFS of the system driven by an optical field with $\Omega = 20\gamma$, $\Delta_L = 0$, and $\omega_s = 40\gamma$ for different values of the parameter G. (a) $G = 0$, (b) $G = 0.5\gamma$, and (c) $G = 2.5\gamma$. (d) Components of the RFS as given in Eq. (28) for the case with $G = 2.5\gamma$.
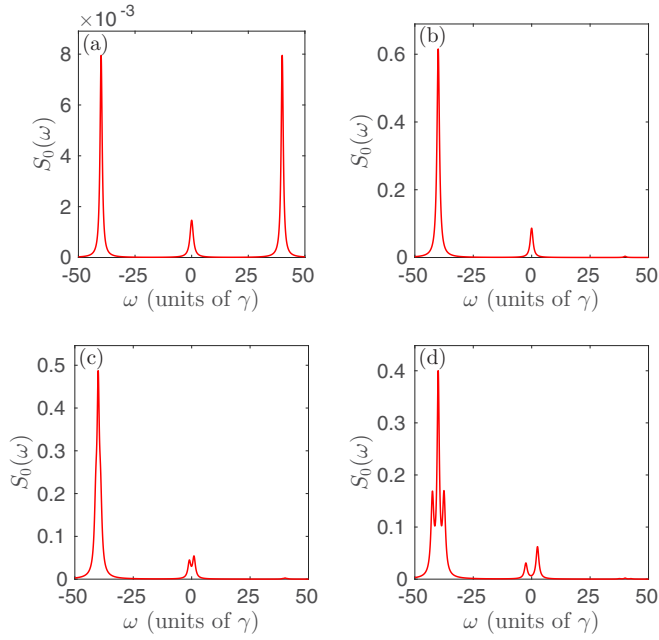
FIG. 5. RFS of the system driven by an optical field with $\Omega = 10\gamma$, $\Delta_L^0 = -34.6\gamma$, and the angular frequency of the LF field is $\omega_s = 40\gamma$. The values of the parameter G are (a) $G = 0$, (b) $G = 0.1\gamma$, (c) $G = \gamma$, and (d) $G = 2.5\gamma$.

behavior whose ultimate origin lies in the fact that at $\Delta_L = 0$ saturation is achieved for whatever value of G [see Fig. 3(d)].

Next, we consider the changes in the RFS obtained when the optical field is detuned from the transition frequency ($\Delta_L \neq 0$) but close to the Rabi resonance condition ($\Delta_q \approx 0$). We have seen in Fig. 3(a) that the Rabi resonance condition is achieved for two different values of Δ_L. Let us consider, for example, the case in which the optical field is tuned at the red detuned Rabi resonance ($\Delta_L^0 = -34.6\gamma$). The results of the numerical calculations for different values of G are shown in Figs. 5(a)–5(d). As for the nonpolar system we recover a Mollow triplet where the central line is depleted with regard to the sidebands. As long as G is different from zero we get an asymmetric spectrum which develops its full structure for the largest value of G. It is worth noting that the level of fluorescent intensity increases up to two orders of magnitude with respect to the nonpolar system. The relevant transitions which produce the red detuned triplet are indicated in Fig. 1(b).

Let us now drive the system slightly out of the Rabi resonance condition. An example of such a situation can be achieved by setting $\Delta_L = \Delta_L^0 + 2\gamma$, such that $\Delta_q \approx +1.7\gamma$; the resulting spectra are shown in Fig. 6. Here, we can devise that the spectrum acquires a high degree of asymmetry; the central line now exhibits a triplet, the red detuned triplet has different peak values for its components, and the blue detuned triplet acquires vanishing components at the largest value of G [see Fig. 6(c)]. As for lower values of G, the different spectral features become spectrally unresolved. This behavior can be understood by taking a closer look at Fig. 3(b). There we can see that for the lowest non-null value of G the system is driven out of the Rabi resonance condition [see the dashed curve in Fig. 3(b)], and population inversion is dramatically reduced with respect to the case with Δ_L^0; thus the peak value of the
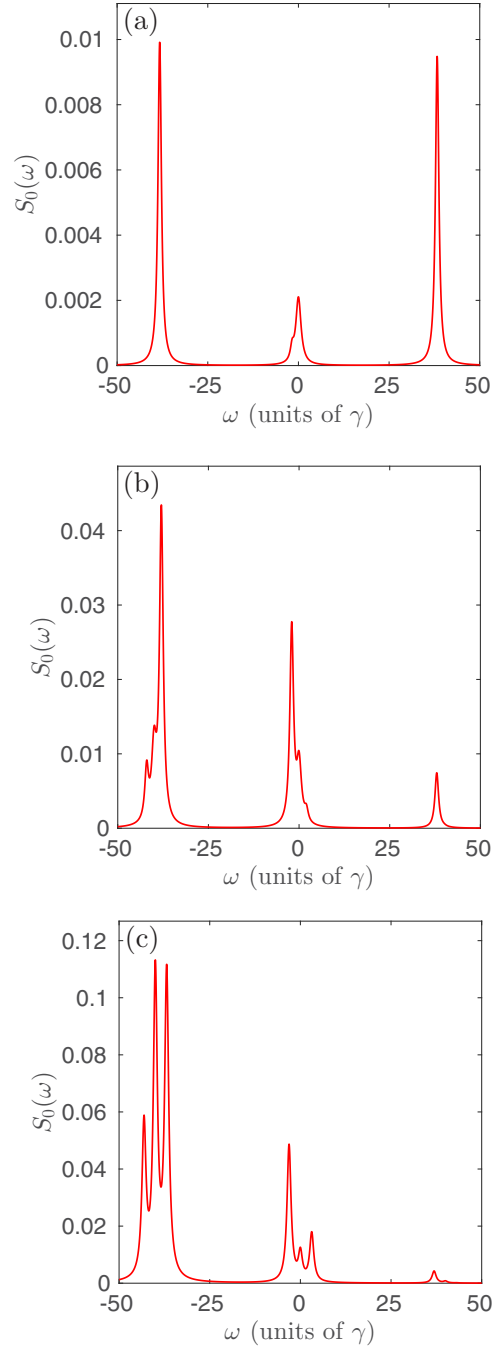
FIG. 6. RFS of the system driven by an optical field with $\Omega = 10\gamma$, $\Delta_L = \Delta_L^0 + 2\gamma$, and the angular frequency of the LF field is $\omega_s = 40\gamma$. The values of the parameter G are (a) $G = 0.1\gamma$, (b) $G = \gamma$, and (c) $G = 2.5\gamma$.

scattered signal of the red detuned spectral feature is strongly suppressed. For the other two values of G, the Rabi resonance depicted in panel 3(b) broadens, resulting in the recovery of the fully resolved red detuned triplet for the largest value of G. Here, the asymmetry arises from the unequal redistribution of populations among the doubly dressed states.

Another way to drive the system out of the Rabi resonance is by changing the angular frequency of the LF field. We have seen in Fig. 3(c) that the change of ω_s shifts the position
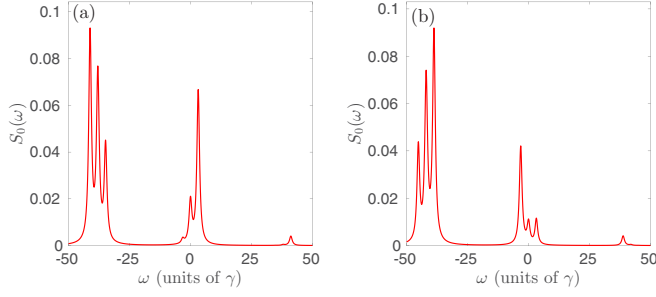
FIG. 7. RFS of the system driven by an optical field with $\Omega = 10\gamma$, $\Delta_L^0 = -34.6\gamma$, and $G = 2.5\gamma$. The angular frequency of the LF field is (a) $\omega_s = 38\gamma$ and (b) $\omega_s = 42\gamma$.

at which the Rabi resonance condition is achieved. Now we consider how the tuning of ω_s allows us to change the RFS of the system. The results of the numerical calculations are depicted in Fig. 7. There we can see that the red detuned triplet, which was originally symmetrical for $\omega_s = 40\gamma$, turns into an

asymmetrical triplet when setting $\omega_s = 42\gamma$ and keeping the rest of the parameters fixed; the original doublet at the center turns into a triplet.

C. Phase-dependent spectrum

In this subsection, we will focus on the influence of the amplitude and frequency of the LF field on the squeezing properties of the quantum system. Usually, the squeezing properties of the fluorescent field in steady state are investigated by analyzing the normally ordered variance $\langle : (\Delta \vec{E}_\theta)^2 : \rangle$, where $\vec{E}_\theta$ is the slowly varying electric-field operator modified due to the beating of the scattered field under study with a local oscillator with phase θ, which is given by

$$\vec{E}_\theta(\vec{r},t) = \tfrac{1}{2}\vec{E}_\theta^+(\vec{r},t)e^{i(\omega_L t+\theta)} + \tfrac{1}{2}\vec{E}_\theta^-(\vec{r},t)e^{-i(\omega_L t+\theta)}$$
$$= \vec{E}_1(\vec{r},t)\cos\theta + \vec{E}_2(\vec{r},t)\sin\theta, \tag{32}$$

where

$$\vec{E}_1(\vec{r},t) = \frac{1}{2}\vec{E}_\theta^+(\vec{r},t)e^{i\omega_L t} + \frac{1}{2}\vec{E}_\theta^-(\vec{r},t)e^{-i\omega_L t}, \tag{33}$$

$$\vec{E}_2(\vec{r},t) = \frac{i}{2}\vec{E}_\theta^+(\vec{r},t)e^{i\omega_L t} - \frac{i}{2}\vec{E}_\theta^-(\vec{r},t)e^{-i\omega_L t} \tag{34}$$

are the in-phase and out-of-phase quadratures of the fluorescent field relative to the local oscillator, respectively. In our case the positive frequency part of the fluorescent light emitted by the quantum system takes the form [64]

$$\vec{E}_\theta^+(\vec{r},t) = f(r)\left[\vec{\mu}_{12}\sigma^-\left(t - \frac{r}{c}\right)\right]e^{-i\omega_L(t-\frac{r}{c})}, \tag{35}$$

where $f(r) = \omega_{21}^2/c^2 r$ and we assume that the detection direction is perpendicular to the dipole moment $\vec{\mu}_{12}$.

Squeezing is characterized by the condition that the normally ordered variance $\langle : (\Delta E_\theta)^2 : \rangle$ of the electric-field quadrature component E_θ is negative. For a two-level system, the normally ordered variance of E_θ was defined in Ref. [17] as

$$\langle :(\Delta E_\theta(\vec{r},t))^2: \rangle = \frac{1}{2\pi}\int_{-\infty}^{\infty}d\omega \int_{-\infty}^{\infty}d\tau\, e^{-i\omega\tau} T\langle \vec{E}_\theta(\vec{r},t),\vec{E}_\theta(\vec{r},t+\tau):\rangle, \tag{36}$$

where $\langle A,B \rangle = \langle AB \rangle - \langle A \rangle\langle B \rangle$ and T is the time-ordering operator. Following Collet *et al.* [65], we introduce the squeezed spectral density

$$\langle :S(\vec{r},t,\theta):\rangle = \frac{1}{2\pi}\int_{-\infty}^{\infty}d\tau\, e^{-i\omega\tau} T\langle : \vec{E}_\theta(\vec{r},t),\vec{E}_\theta(\vec{r},t+\tau):\rangle. \tag{37}$$

Inserting the positive and negative parts of the fluorescent field (35) into Eq. (37), we can express the spectrum as

$$\langle :S(\vec{r},t,\theta):\rangle = \mu_{12}^2 \frac{f^2(r)}{4\pi}\text{Re}\int_0^{\infty}d\tau(e^{i\omega\tau} + e^{-i\omega\tau})[\langle\delta\sigma^-(t+\tau),\delta\sigma^-(t)\rangle e^{i(2\theta+\omega_L r/c)} + \langle\delta\sigma^+(t+\tau),\delta\sigma^-(t)\rangle]. \tag{38}$$

As in the case of the RFS, for the squeezing spectrum, it is necessary to evaluate two correlation functions, namely, $\langle\delta\sigma^+(t+\tau)\cdot\delta\sigma^-(t)\rangle$, which has already been evaluated in Eq. (26), and a new correlation term given by $\langle\delta\sigma^-(t+\tau)\cdot\delta\sigma^-(t)\rangle$, which is essential for squeezing. After a lengthy but straightforward calculation we can arrive at an analytical expression for the squeezing spectrum, $S_\theta(\omega)$:

$$S_\theta(\omega) = \text{Re}\big[\big(S_{(zz)}^\theta + S_{(+-)}^\theta + S_{(-+)}^\theta\big)e^{2i\theta} + S_0(\omega) + S_0(-\omega)\big], \tag{39}$$

where

$$S_{(zz)}^\theta(\omega) = S_{00}\left[\sum_n\left(\frac{1}{\gamma_2 - i[\omega - \omega_L + (q+n)\omega_s]} + \frac{1}{\gamma_2 + i[\omega - \omega_L - (q+n)\omega_s]}\right)D_1 + \sum_n\left(\frac{1}{\gamma_2 - i[\omega - \omega_L - (q+n)\omega_s]}\right.\right.$$

$$\left.\left. + \frac{1}{\gamma_2 + i[\omega - \omega_L + (q+n)\omega_s]}\right)D_2 + \left(\frac{1}{\gamma_2 - i(\omega - \omega_L)} + \frac{1}{\gamma_2 + i(\omega - \omega_L)}\right)D_3\right], \tag{40}$$

$$S_{(+-)}^{\theta}(\omega) = S_{0+} \left[\sum_n \left(\frac{1}{\Gamma_s - i[\omega - \omega_L + (q+n)\omega_s + \Omega_s]} + \frac{1}{\Gamma_s + i[\omega - \omega_L - (q+n)\omega_s - \Omega_s]} \right) E_1 \right.$$

$$+ \sum_n \left(\frac{1}{\Gamma_s - i[\omega - \omega_L - (q+n)\omega_s + \Omega_s]} + \frac{1}{\Gamma_s + i[\omega - \omega_L + (q+n)\omega_s - \Omega_s]} \right) E_2$$

$$\left. + \left(\frac{1}{\Gamma_s - i(\omega - \omega_L + \Omega_s)} + \frac{1}{\Gamma_s + i(\omega - \omega_L - \Omega_s)} \right) E_3 \right], \tag{41}$$

$$S_{(-+)}^{\theta}(\omega) = S_{0-} \left[\sum_n \left(\frac{1}{\Gamma_s - i[\omega - \omega_L + (q+n)\omega_s - \Omega_s]} + \frac{1}{\Gamma_s + i[\omega - \omega_L - (q+n)\omega_s + \Omega_s]} \right) F_1 \right.$$

$$+ \sum_n \left(\frac{1}{\Gamma_s - i[\omega - \omega_L - (q+n)\omega_s - \Omega_s]} + \frac{1}{\Gamma_s + i[\omega - \omega_L + (q+n)\omega_s + \Omega_s]} \right) F_2$$

$$\left. + \left(\frac{1}{\Gamma_s - i(\omega - \omega_L - \Omega_s)} + \frac{1}{\Gamma_s + i(\omega - \omega_L + \Omega_s)} \right) F_3 \right], \tag{42}$$

where $S_{00} = \frac{1 - \langle S_z(\infty) \rangle^2}{4}$ and $S_{0\pm} = \frac{1 \pm \langle S_z(\infty) \rangle}{8}$. Note that $S_0(\pm\omega)$ has been defined in Eq. (28), and the coefficients D_j, E_j, and F_j are explicitly given in Appendix B.

We assume that $e^{-i\omega_L(t - \frac{r}{c})} = 1$ and scale the spectrum in Eq. (38) to $\mu_{12}^2 \frac{f^2(r)}{4\pi}$. We consider the case of moderate driving close to the condition of Rabi resonance such that the Rabi frequency of the control field is $\Omega = 10\gamma$ and the optical field is assumed to be far detuned $\Delta_L^0 = -34.6\gamma$. The angular frequency of the LF field is set to $\omega_s = 40\gamma$ [in Figs. 8(a) and 8(b)], where the Rabi resonance condition is met, or to $\omega_s = 42\gamma$ [in Figs. 8(c) and 8(d)], which is slightly out of the

Rabi resonance. The value of the parameter G is selected to be $G = 2.5\gamma$. Solid curves in Figs. 8(a) and 8(b) show the results for the in-phase and out-of-phase quadratures when the system is at the Rabi resonance condition. Here, we can devise that the level of fluctuations is always positive for all the range of frequencies in contrast to the case of a nonpolar two-level atom shown with dashed curves. This result can be understood if we realize that in the nonpolar case the level of population in the excited state is vanishingly small [as indicated with dashed curve in Fig. 3(b)] at $\Delta_L^0 = -34.6\gamma$, in contrast to the case of the polar system driven by a LF field where at such value of the optical detuning we get the Rabi resonance
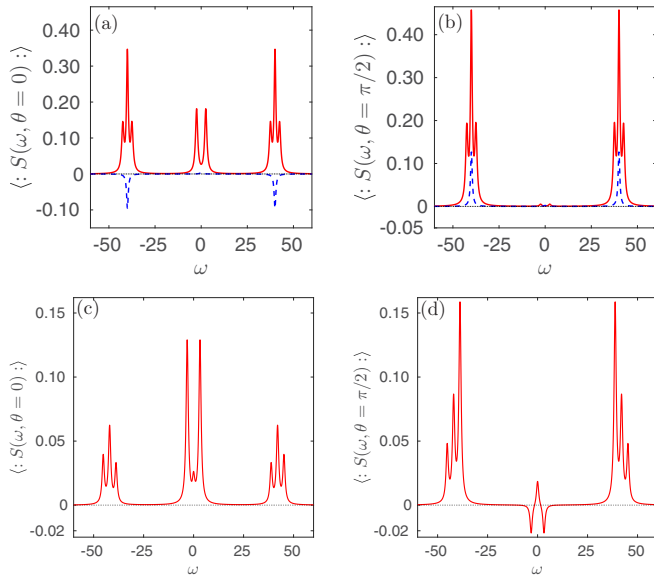
FIG. 8. Squeezing spectrum of the fluorescent field for the in-phase [(a)–(c)] and out-of-phase [(b)–(d)] quadratures when the system is driven such that $\Omega = 10\gamma$, $\Delta_L^0 = -34.6\gamma$, $G = 2.5\gamma$ with $\omega_s = 40\gamma$ [(a),(b)] and $\omega_s = 42\gamma$ [(c),(d)]. The dashed curves in (a),(b) correspond to the results obtained in a nonpolar two-level atom.
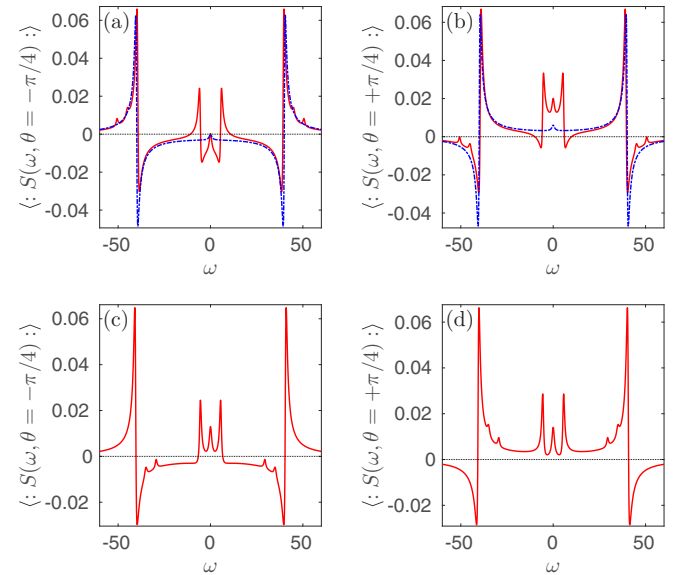
FIG. 9. Squeezing spectrum of the fluorescent field for different quadratures: $\theta = -\pi/4$ [(a)–(c)]; $\theta = +\pi/4$ [(b)–(d)]. The system is driven such that $\Omega = 10\gamma$, $\Delta_L^0 = -34.6\gamma$, $G = 2.5\gamma$; $\omega_s = 45\gamma$ in (a),(b) and $\omega_s = 35\gamma$ in (c),(d). The dashed curves in (a),(b) correspond to the results obtained in a nonpolar two-level atom.

peak and the system is close to saturation [dotted curve in Fig. 3(b)]. This in turn manifests in a high level of noise due to spontaneous emission in the latter case. However, the situation changes when $\omega_s = 42\gamma$ while keeping constant the rest of the parameters as shown in Figs. 8(c) and 8(d). Here, we obtain squeezing at the sidebands of the central triplet located at $\pm\Omega_s$, a situation which differs from the one found in a conventional two-level system without PDMs.

A wide variety of features can be obtained when considering other quadratures of the fluorescent field. We present the results obtained for two different values of ω_s as solid curves in Fig. 9 and with $\theta = \pi/4$, whereas the dashed curves correspond to the non-polar case. There we clearly see that a reduced level of fluctuations is produced at other frequencies compared to the case analyzed in Fig. 8. Note that, in all cases in Fig. 9, the strong driven-laser detuning Δ_L is kept constant and it is solely the change in the frequency of the LF field that is responsible for the significant squeezing spectrum tuning. In summary, we can control the spectral region where squeezing is obtained through the changes in the intensity and frequency of the LF field in a nonpolar system.

IV. CONCLUSIONS

In this work we presented a theoretical description of the interaction of a polar quantum system with an optical field, which drives the electronic transition, and is simultaneously subjected to a second LF field that couples to the PDMs. Using a series of unitary transformations we have derived a master equation for the reduced density matrix which is valid for the case of weak modulation near the Rabi resonance. Using parameters for a specific molecular system, we have analyzed the steady-state population inversion in the strong and moderate regimes for the optical field. When the angular frequency of the LF field is chosen close to the Rabi frequency of the optical field the system reaches a resonance condition close to saturation in spite of the optical field being far detuned. New features in the RFS have been obtained with the emergence of a series of Mollow triplets. In addition,

we have analyzed the squeezing spectrum of the fluorescent field where a reduced level of fluctuations is found at certain sidebands. The spectral location and the height of the different sidebands can be tailored through the intensity and angular frequency of the LF field. It is worth mentioning that the theoretical description presented in this work is not restricted to the particular type of molecular complex used to illustrate the optical behavior of the polar system but can be applied to various quantum systems with broken inversion symmetry such as asymmetric QDs and superconducting qubits. These studies are of interest due to their potential applications in quantum information technologies [66–68], as well as in quantum amplifiers and attenuators [69].

APPENDIX A: DERIVATION OF THE EFFECTIVE HAMILTONIAN

The eigenstates of $H^{(01)}$ are the so-called dressed states of the combined quantum system–strong laser field and are given by

$$|\overline{\alpha}\rangle = \cos(\theta)|2\rangle + \sin(\theta)|1\rangle,$$
$$|\overline{\beta}\rangle = -\sin(\theta)|2\rangle + \cos(\theta)|1\rangle. \tag{A1}$$

The operators R^+, R^+, and R_z appearing in Eq. (10) are related with the bare operators through

$$\hat{\sigma}^+ = \tfrac{1}{2}\sin(2\theta)R_z + \cos^2(\theta)R^+ - \sin^2(\theta)R^-,$$
$$\hat{\sigma}^- = \tfrac{1}{2}\sin(2\theta)R_z + \cos^2(\theta)R^- - \sin^2(\theta)R^+, \tag{A2}$$
$$\hat{\sigma}_z = \cos(2\theta)R_z - \sin(2\theta)(R^+ + R^-).$$

Then, we assume the resonance condition: $\Delta_q \equiv \Omega_R - q\omega_s \ll \omega_s$, with q being an integer. This allows one to rewrite Eq. (12) as

$$H^{(3)} = -\hbar G c_1 s_1 \Bigg\{ \sum_l J_l(z)[R^+ e^{i[\Delta_q + (l+q-1)\omega_s]t} + R^- e^{-i[\Delta_q + (l+q-1)\omega_s]t}]$$

$$+ \sum_l J_l(z)[R^+ e^{i[\Delta_q + (l+q+1)\omega_s]t} + R^- e^{-i[\Delta_q + (l+q+1)\omega_s]t}] \Bigg\}$$

$$+ \hbar U_3^\dagger(t) \sum_k g_k \big[a_k^\dagger e^{i(\omega_k - \omega_L)t} (c_1 s_1 R_z + c_1^2 R^- - s_1^2 R^+) + \text{H.a.} \big] U_3(t). \tag{A3}$$

In the spirit of the RWA we only keep the slow oscillating terms, i.e., we consider $l + q - 1 = 0$ in the first sum and $l + q + 1 = 0$ in the second sum. Therefore, Eq. (A3) simplifies to

$$H^{(3)} = -\hbar G \sin(2\theta)(-1)^{q+1} \frac{2q J_q(z)}{z} (R^+ e^{i\Delta_q t} + R^- e^{-i\Delta_q t})$$

$$+ \hbar U_3^\dagger(t) \sum_k g_k \big[a_k^\dagger e^{i(\omega_k - \omega_L)t} (c_1 s_1 R_z + c_1^2 R^- - s_1^2 R^+) + \text{H.a.} \big] U_3(t). \tag{A4}$$

In the following we remove the oscillating terms in the coherent part of the Hamiltonian in Eq. (A4) by using the following unitary transformation: $U_4 = e^{i\frac{\Delta_s}{2} t R_z}$. The new Hamiltonian reads $H^{(4)} = H_{\text{ext}}^{(4)} + V^{(4)}$, and it is given by

$$H_{\text{ext}}^{(4)} = \frac{\hbar \Delta_q}{2} R_z - \hbar G \, \sin(2\theta)(-1)^{q+1} \frac{2q J_q(z)}{z}(R^+ + R^-), \quad V^{(4)} = \hbar \sum_k [a_k^\dagger F_k(t) + F_k^\dagger a_k], \tag{A5}$$

where

$$F_k(t) = g_k c_1 s_1 e^{i(\omega_k - \omega_L)t} R_z + \sum_l g_k J_l(z)\big[c_1^2 R^- e^{i(\omega_k + \Delta_q - \omega_L - \Omega_R - l\,\omega_s)t} - s_1^2 R^+ e^{i(\omega_k - \Delta_q - \omega_L + \Omega_R + l\,\omega_s)t}\big]. \tag{A6}$$

The first line in Eq. (A5) contains the interaction of the quantum system with the driving laser fields while the second term accounts for the interaction of the quantum system with the vacuum reservoir.

Having derived the effective interaction Hamiltonian, we now turn to obtaining the effective Lindblad master equation for the reduced density operator of the quantum system. To this end we trace the density matrix of the total system over the bath variables which is assumed to be a standard reservoir at null temperature. The density matrix of the quantum system to second order of perturbation and assuming the Born-Markoff approximation [63] results in

$$\frac{\partial \rho^{(4)}}{\partial t} = -\frac{i}{\hbar}\big[H_{\text{ext}}^{(4)}, \rho^{(4)}\big] - \frac{1}{\hbar^2}\text{Tr}_B \int_0^t dt' [V^{(4)}(t)V^{(4)}(t')\rho^{(4)}\Gamma_B - V^{(4)}(t)\rho^{(4)}\Gamma_B V^{(4)}(t') + \text{H.a.}]. \tag{A7}$$

We finally obtain the following master equation:

$$\frac{\partial \rho^{(4)}(t)}{\partial t} = -i\frac{\Delta_q}{2}[R_z, \rho^{(4)}] + i\left(G\sin(2\theta)(-1)^{q+1}\frac{2q J_q(z)}{z}\right)[R^+ + R^-, \rho^{(4)}] + L\rho^{(4)}, \tag{A8}$$

with the Liouvillian $L\rho^{(4)}$ given by

$$L\rho^{(4)} = -\frac{\gamma_0}{2}[R_z R_z \rho - R_z \rho R_z + \text{H.a.}]$$
$$- \frac{\gamma_+}{2}[R^+ R^- \rho - R^- \rho R^+ + \text{H.a.}]$$
$$- \frac{\gamma_-}{2}[R^- R^+ \rho - R^+ \rho R^- + \text{H.a.}]. \tag{A9}$$

The effective decay rates are given by

$$\gamma_0 = s_1^2 c_1^2 \gamma(\omega_L),$$
$$\gamma_+ = c_1^4 \sum_l \gamma(\omega_L + \Omega_R + l\omega_s)J_l^2(z), \tag{A10}$$
$$\gamma_- = s_1^4 \sum_l \gamma(\omega_L - \Omega_R - l\omega_s)J_l^2(z),$$

where $\gamma(\omega_L) = 2\pi \sum_k g_k^2 \delta(\omega_k - \omega_L)$. Here γ_+ represents the transition rate from the upper dressed state $|\overline{\alpha}\rangle$ to the lower dressed state $|\overline{\beta}\rangle$, and γ_- denotes the transition rate from $|\overline{\beta}\rangle$ to $|\overline{\alpha}\rangle$. In the regime where $\omega_s, \Omega_R \ll \omega_L$, we can assume that $\gamma[\omega_L \pm (\Omega_R + l\omega_s)] \approx \gamma(\omega_L) \equiv \gamma$.

Equation (A8) resembles the results derived in Ref. [57]. Magnitude $\overline{\Delta}$ in Ref. [57] stands for our Δ_q, while for the effective Rabi frequency $\overline{G}$ in Ref. [57] we obtain $G\sin(2\theta)(-1)^{q+1}\frac{2q J_q(z)}{z}$. In our approach, we allow the LF field to exchange q photons with the optical field. Furthermore, the effective decay rates in Eq. (A10) differ from the ones derived in Ref. [57] in the weighting factors involving Bessel functions.

Since we are interested in the physics in the strong-driving regime, we move to the double-dressed picture in order to simplify the analytical results. To do this we diagonalize the Hamiltonian $H^{(4)}$ in Eq. (A5) by means of a rotation operator $U_5 = e^{-i\phi\sigma_y}$, where $\sin(2\phi) = -\frac{\Delta_q}{\Omega_S}$, $\cos(2\phi) = \frac{2\Omega_R}{\Omega_S}$,

and $\Omega_S \equiv \sqrt{\Delta_q^2 + (2\Omega_R)^2}$. Then, the transformed matrix density $\rho^{(5)}(t)$ satisfies Eq. (13).

APPENDIX B: ANALYTICAL DERIVATION OF THE RESONANCE FLUORESCENCE AND THE PHASE-DEPENDENT SPECTRA SCATTERED BY THE DOUBLE-DRESSED MOLECULE

To obtain the resonance fluorescence and squeezing spectra we have to evaluate the integrals in Eq. (25) and in Eq. (37) in the steady-state limit. The starting point is the result indicated in Eq. (27). It is easy to show that the only nonzero correlations between the operators in the doubly dressed basis are $\langle \delta S_z(t + \tau)\delta S_z(t)\rangle$, $\langle \delta S^+(t + \tau)\delta S^-\rangle$, and $\langle \delta S^-(t + \tau)\delta S^+(t)\rangle$. This is due to the fact that $\langle \delta S^+(t)\rangle = \langle \delta S^+(t)\rangle = 0$ at steady state [see Eq. (18)]. Here, $\langle \delta S_\mu(\tau)\delta S_\nu(0)\rangle = \text{Tr}[\delta S_\mu(\tau)\delta S_\nu(0)\rho]$ ($\mu, \nu = z, +, -$). Thus the correlation function $\langle \delta \sigma^+(t + \tau)\delta \sigma^-(t)\rangle$ can be recast as

$$\langle \delta\sigma^+(t)\delta\sigma^-(t')\rangle = F_{zz}(t,t')\langle \delta S_z(t)\delta S_z(t')\rangle$$
$$+ F_{+-}(t,t')\langle \delta S^+(t)\delta S^-(t')\rangle$$
$$+ F_{-+}(t,t')\langle \delta S^-(t)\delta S^+(t')\rangle, \tag{B1}$$

where the functions $F_{zz}(t,t')$, $F_{+-}(t,t')$, and $F_{-+}(t,t')$ are given by

$$F_{zz}(t,t')$$
$$= a_{11}Y_{nq}(t)Y_{mq}(t') + a_{12}Y_{nq}(t)Y_{mq}(-t') + a_{13}Y_{nq}(t')$$
$$+ a_{21}Y_{nq}(-t)Y_{mq}(t') + a_{22}Y_{nq}(-t)Y_{mq}(-t')$$
$$+ a_{23}Y_{nq}(-t')a_{31}Y_{nq}(t') + a_{32}Y_{nq}(-t') + a_{33}e^{i\omega_L(t-t')},$$

$$F_{+-}(t,t')$$
$$= b_{11}Y_{nq}(t)Y_{mq}(t') + b_{12}Y_{nq}(t)Y_{mq}(-t') + b_{13}Y_{nq}(t')$$

$$+ b_{21}Y_{nq}(-t)Y_{mq}(t') + b_{22}Y_{nq}(-t)Y_{mq}(-t')$$
$$+ b_{23}Y_{nq}(-t')b_{31}Y_{nq}(t') + b_{32}Y_{nq}(-t') + b_{33}e^{i\omega_L(t-t')},$$

$$F_{-+}(t,t')$$
$$= c_{11}Y_{nq}(t)Y_{mq}(t') + c_{12}Y_{nq}(t)Y_{mq}(-t') + c_{13}Y_{nq}(t')$$
$$+ c_{21}Y_{nq}(-t)Y_{mq}(t') + c_{22}Y_{nq}(-t)Y_{mq}(-t')$$
$$+ c_{23}Y_{nq}(-t')c_{31}Y_{nq}(t') + c_{32}Y_{nq}(-t') + c_{33}e^{i\omega_L(t-t')}.$$

(B2)

The coefficients a_{ij}, b_{ij}, and c_{ij} are given by

$$a_{11} = \frac{\sin^2(2\phi)[\cos(2\theta) + 1][\cos(2\theta) - 1]}{4},$$

$$a_{12} = \frac{\sin^2(2\phi)[\cos(2\theta) + 1]^2}{4},$$

$$a_{13} = \frac{\sin(2\theta)[\cos(2\theta) + 1]\sin(2\phi)\cos(2\phi)}{2},$$

$$a_{21} = \frac{[\cos(2\theta) - 1]^2 \sin^2(2\phi)}{4},$$

$$a_{22} = \frac{(\cos(2\theta) + 1)(\cos(2\theta) - 1)\sin^2(2\phi)}{4},$$

$$a_{23} = \frac{\sin(2\theta)[\cos(2\theta) - 1]\sin(2\phi)\cos(2\phi)}{2},$$

$$a_{31} = \frac{\sin(2\theta)[\cos(2\theta) - 1]\sin(2\phi)\cos(2\phi)}{2},$$

$$a_{32} = \frac{\sin(2\theta)[\cos(2\theta) + 1]\sin(2\phi)\cos(2\phi)}{2},$$

$$a_{33} = \sin^2(2\theta)\cos^2(2\phi),$$

(B3)

$$b_{11} = \frac{[\cos(2\theta) + 1][\cos(2\theta) - 1][\cos(2\phi) + 1][\cos(2\phi) - 1]}{4},$$

$$b_{12} = \frac{[\cos(2\theta) + 1]^2[\cos(2\phi) + 1]^2}{4},$$

$$b_{13} = -\frac{\sin(2\theta)\sin(2\phi)[\cos(2\theta) + 1][\cos(2\phi) + 1]}{2},$$

$$b_{21} = \frac{[\cos(2\theta) - 1]^2[\cos(2\phi) - 1]^2}{4},$$

$$b_{22} = \frac{[\cos(2\theta) - 1][\cos(2\theta) + 1][\cos(2\phi) - 1][\cos(2\phi) + 1]}{4},$$

$$b_{23} = -\frac{\sin(2\theta)\sin(2\phi)[\cos(2\theta) - 1][\cos(2\phi) - 1]}{2},$$

$$b_{31} = -\frac{\sin(2\theta)\sin(2\phi)[\cos(2\theta) - 1][\cos(2\phi) - 1]}{2},$$

$$b_{32} = -\frac{\sin(2\theta)\sin(2\phi)[\cos(2\theta) + 1][\cos(2\phi) + 1]}{2},$$

$$b_{33} = \sin^2(2\theta)\sin^2(2\phi),$$

(B4)

$$c_{11} = \frac{[\cos(2\theta) + 1][\cos(2\theta) - 1][\cos(2\phi) + 1][\cos(2\phi) - 1]}{4},$$

$$c_{12} = \frac{[\cos(2\theta) + 1]^2[\cos(2\phi) - 1]^2}{4},$$

$$c_{13} = -\frac{\sin(2\theta)\sin(2\phi)[\cos(2\theta) + 1][\cos(2\phi) - 1]}{2},$$

$$c_{21} = \frac{[\cos(2\theta) - 1]^2[\cos(2\phi) + 1]^2}{4},$$

$$c_{22} = \frac{[\cos(2\theta) - 1][\cos(2\theta) + 1][\cos(2\phi) - 1][\cos(2\phi) + 1]}{4},$$

$$c_{23} = -\frac{\sin(2\theta)\sin(2\phi)[\cos(2\theta) - 1][\cos(2\phi) + 1]}{2},$$

$$c_{31} = -\frac{\sin(2\theta)\sin(2\phi)[\cos(2\theta) - 1][\cos(2\phi) + 1]}{2},$$

$$c_{32} = -\frac{\sin(2\theta)\sin(2\phi)[\cos(2\theta) + 1][\cos(2\phi) - 1]}{2},$$

$$c_{33} = \sin^2(2\theta)\sin^2(2\phi).$$

(B5)

Once the correlation function has been obtained, the RFS can be determined through

$$S(\omega) = \lim_{t \to \infty} \frac{1}{T} \int_0^T dt \int_0^T dt' \langle \delta\sigma^+(t)\delta\sigma^-(t')\rangle e^{-i\omega(t-t')}$$
$$= S_{(zz)}(\omega) + S_{(+-)}(\omega) + S_{(-+)}(\omega),$$

(B6)

where

$$S_{(zz)}(\omega) = \lim_{t \to \infty} \frac{1}{T} \int_0^T dt \int_0^T dt' [F_{zz}(t,t')\langle \delta S_z(t)\delta S_z(t')\rangle]e^{-i\omega(t-t')},$$

$$S_{(+-)}(\omega) = \lim_{t \to \infty} \frac{1}{T} \int_0^T dt \int_0^T dt' [F_{+-}(t,t')\langle \delta S^+(t)\delta S^-(t')\rangle]e^{-i\omega(t-t')},$$

(B7)

$$S_{(-+)}(\omega) = \lim_{t \to \infty} \frac{1}{T} \int_0^T dt \int_0^T dt' [F_{-+}(t,t')\langle \delta S^-(t)\delta S^+(t')\rangle]e^{-i\omega(t-t')}.$$

When evaluating the spectrum $S(\omega)$, we have to carry out integrals of the type

$$I_{nm}(\omega) \equiv \lim_{t \to \infty} \frac{1}{T} \int_0^T dt \int_0^T dt' Y_{nq}(t)Y_{mq}(t')\langle S_\mu(t)S_\nu(t')\rangle e^{-i\omega(t-t')}$$
$$= \lim_{t \to \infty} \frac{1}{T} \sum_n \sum_m \int_0^T dt \int_0^T dt' J_n(z)e^{i(n+q)\omega_s t}J_m(z)e^{i(m+q)\omega_s t'}\langle \delta S_\mu(t)\delta S_\nu(t')\rangle e^{-i(\omega-\omega_L)(t-t')}.$$

(B8)

When making the substitution $t - t' = \tau$, the integral becomes

$$I_{nm}(\omega) = \lim_{t \to \infty} \frac{1}{T} \sum_n \sum_m \int_0^T dt' \, J_n(z) J_m(z) e^{i(n+m+2q)\omega_s t'} \int_0^T d\tau \, \langle S_\mu(t) S_\nu(t') \rangle e^{-i[\omega - \omega_L - (q+n)\omega_s]\tau}$$

$$= \sum_n \sum_m J_n(z) J_m(z) \delta_{n,-(m+2q)} \int_0^T d\tau \, \langle \delta S_\mu(\tau) \delta S_\nu(0) \rangle e^{-i[\omega - \omega_L - (q+n)\omega_s]\tau}$$

$$= \sum_n J_n(z) J_{-(n+2q)}(z) \int_0^T d\tau \, \langle \delta S_\mu(\tau) \delta S_\nu(0) \rangle e^{-i[\omega - \omega_L - (q+n)\omega_s]\tau}. \tag{B9}$$

Using this result, one can easily show that the first term in Eq. (B7) is given by

$$S_{zz}(\omega) = \text{Re} \int_0^\infty d\tau \left[a_{11} \sum_n (-1)^{(n+2q)} J_n(z) J_{n+2q}(z) e^{i(q+n)\omega_s \tau} + a_{12} \sum_n J_n^2(z) e^{i(q+n)\omega_s \tau} e^{-i(\omega - \omega_L)\tau} a_{13} J_{-q}(z) \right.$$

$$+ a_{21} \sum_n J_n^2(z) e^{-i(q+n)\omega_s \tau} + a_{22} \sum_n (-1)^{(n+2q)} J_n(z) J_{n+2q}(z) e^{-i(q+n)\omega_s \tau} a_{23} J_{-q}(z)$$

$$\left. + a_{31} J_{-q}(z) + a_{32} J_{-q}(z) + a_{33} \right] e^{-i(\omega - \omega_L)\tau} \langle \delta S_z(\tau) \delta S_z(0) \rangle, \tag{B10}$$

and similar expressions for $S_{+-}(\omega)$ and $S_{-+}(\omega)$, namely

$$S_{+-}(\omega) = \text{Re} \int_0^\infty d\tau \left[b_{11} \sum_n (-1)^{(n+2q)} J_n(z) J_{n+2q}(z) e^{i(q+n)\omega_s \tau} + b_{12} \sum_n J_n^2(z) e^{i(q+n)\omega_s \tau} e^{-i(\omega - \omega_L)\tau} b_{13} J_{-q}(z) \right.$$

$$+ b_{21} \sum_n J_n^2(z) e^{-i(q+n)\omega_s \tau} + b_{22} \sum_n (-1)^{(n+2q)} J_n(z) J_{n+2q}(z) e^{-i(q+n)\omega_s \tau} b_{23} J_{-q}(z)$$

$$\left. + b_{31} J_{-q}(z) + b_{32} J_{-q}(z) + b_{33} \right] e^{-i(\omega - \omega_L)\tau} \langle \delta S^+(\tau) \delta S^-(0) \rangle, \tag{B11}$$

$$S_{-+}(\omega) = \text{Re} \int_0^\infty d\tau \left[c_{11} \sum_n (-1)^{(n+2q)} J_n(z) J_{n+2q}(z) e^{i(q+n)\omega_s \tau} + c_{12} \sum_n J_n^2(z) e^{i(q+n)\omega_s \tau} e^{-i(\omega - \omega_L)\tau} c_{13} J_{-q}(z) \right.$$

$$+ c_{21} \sum_n J_n^2(z) e^{-i(q+n)\omega_s \tau} + c_{22} \sum_n (-1)^{(n+2q)} J_n(z) J_{n+2q}(z) e^{-i(q+n)\omega_s \tau} c_{23} J_{-q}(z)$$

$$\left. + c_{31} J_{-q}(z) + c_{32} J_{-q}(z) + c_{33} \right] e^{-i(\omega - \omega_L)\tau} \langle \delta S^-(\tau) \delta S^+(0) \rangle. \tag{B12}$$

To obtain the explicit expression for the spectrum, it is necessary to evaluate the correlation function $\langle \delta S\mu(\tau) \delta S_\nu(0) \rangle$ ($\mu, \nu = z, +, -$). To do that it is practical to define the column vector

$$\hat{U}^{(k)}(\tau) = [\langle \delta S^+(\tau) \delta S^k(0) \rangle, \langle \delta S^-(\tau) \delta S^k(0) \rangle, \langle \delta S^z(\tau) \delta S^k(0) \rangle]^T, \tag{B13}$$

where superindex T stands for transpose and $k = +, -, z$. According to the quantum regression theorem the vector $\hat{U}^k(\tau)$ satisfies

$$\frac{d}{d\tau} \hat{U}^{(k)}(\tau) = M \hat{U}^{(k)}(\tau), \tag{B14}$$

where the matrix M is given by

$$M = \begin{pmatrix} -(\Gamma_s - i\Omega_s) & 0 & 0 \\ 0 & -(\Gamma_s + i\Omega_s) & 0 \\ 0 & 0 & -\gamma_2 \end{pmatrix}. \tag{B15}$$

When the solution of Eq. (B14) is introduced in Eqs. (B10)–(B12) we obtain the RFS spectrum given in Eqs. (29)–(31) in the manuscript, where the coefficients A_j, B_j, C_j $j = 1, 2, 3$ are given by

$$A_1 = a_{11} J_n(z) J_{n+2q}(z) + a_{12} J_n^2(z), \quad A_2 = a_{21} J_n^2(z) + a_{12} J_n(z) J_{n+2q}(z), \quad A_3 = (a_{13} + a_{23} + a_{31} + a_{32}) J_{-q}(z) + a_{33}. \tag{B16}$$

The expressions for $B_j(C_j)$ are obtained from A_j in Eq. (B16) by making the replacement $a_{ij} \to b_{ij}(\to c_{ij})$.

In a similar way we can obtain the squeezing spectrum. In doing that we follow Ref. [65] where the squeezed spectral density is defined as

$$\langle :S(\vec{r}, t, \theta): \rangle = \frac{1}{2\pi} \int_{-\infty}^\infty d\tau \, e^{-i\omega\tau} T \langle :E_\theta(\vec{r}, t), E_\theta(\vec{r}, t + \tau): \rangle. \tag{B17}$$

Taking into account the action of the time-ordering operator T, the integrand of Eq. (B17) reduces to

$$T\langle :E_\theta(\vec{r},t),E_\theta(\vec{r},t+\tau):\rangle = \tfrac{1}{4}(\langle \vec{E}_\theta^+(\vec{r},t+\tau),\vec{E}_\theta^+(\vec{r},t)\rangle e^{i\omega_L(2t+\tau+2\theta)} + \langle \vec{E}_\theta^-(\vec{r},t+\tau),\vec{E}_\theta^-(\vec{r},t)\rangle e^{-i\omega_L(2t+\tau+2\theta)}$$

$$+ \langle \vec{E}_\theta^+(\vec{r},t+\tau),\vec{E}_\theta^-(\vec{r},t)\rangle e^{i\omega_L\tau} + \langle \vec{E}_\theta^-(\vec{r},t+\tau),\vec{E}_\theta^+(\vec{r},t)\rangle e^{-i\omega_L\tau}). \tag{B18}$$

Inserting the positive and negative parts of the fluorescent field given in Eq. (35) into Eq. (B18) and the result in Eq. (B17), the squeezing spectrum in the bare basis takes the form

$$\langle :S(\vec{r},t,\theta):\rangle = \mu_{12}^2 \frac{f^2(r)}{4\pi} \mathrm{Re} \int_0^\infty d\tau (e^{i\omega\tau} + e^{-i\omega\tau})[\langle \delta\sigma^-(t+\tau),\delta\sigma^-(t)\rangle e^{i(2\theta+2\omega_L r/c)} + \langle \delta\sigma^+(t+\tau),\delta\sigma^-(t)\rangle]. \tag{B19}$$

Note that integrand in Eq. (B19) contains the correlation function $\langle \delta\sigma^+(t+\tau)\delta\sigma^-(t)\rangle$ which has been already calculated, and an additional correlation $\langle \delta\sigma^-(t+\tau)\delta\sigma^-(t)\rangle$. For the evaluation of the latter we follow the same steps as above and finally arrive at the result given in Eqs. (40)–(42) of the manuscript, where the coefficients d_{ij}, e_{ij}, and f_{ij} read

$$d_{11} = \frac{[\cos(2\theta) - 1]^2 \sin^2(2\phi)}{4},$$

$$d_{12} = \frac{[\cos(2\theta) + 1][\cos(2\phi) - 1]\sin^2(2\phi)}{4},$$

$$d_{13} = -\frac{[\cos(2\theta) - 1]\sin(2\theta)\sin(2\phi)\cos(2\phi)}{2},$$

$$d_{21} = \frac{[\cos(2\theta) + 1][\cos(2\theta) - 1]\sin^2(2\phi)}{4},$$

$$d_{22} = \frac{[\cos(2\theta) + 1]^2 \sin^2(2\phi)}{4},$$

$$d_{23} = \frac{[\cos(2\theta) + 1]\sin(2\theta)\sin(2\phi)\cos(2\phi)}{2},$$

$$d_{31} = \frac{[\cos(2\theta) - 1]\sin(2\theta)\sin(2\phi)\cos(2\phi)}{4},$$

$$d_{32} = \frac{[\cos(2\theta) + 1]\sin(2\phi)\sin(2\theta)\cos(2\phi)}{4},$$

$$d_{33} = \sin^2(2\theta)\cos^2(2\phi), \tag{B20}$$

$$e_{11} = \frac{[\cos(2\theta) - 1]^2[\cos(2\phi) + 1][\cos(2\phi) - 1]}{4},$$

$$e_{12} = \frac{[\cos(2\theta) - 1][\cos(2\theta) + 1][\cos(2\phi) + 1]^2}{4},$$

$$e_{13} = -\frac{[\cos(2\theta) - 1][\cos(2\phi) + 1]\sin(2\theta)\sin(2\phi)}{2},$$

$$e_{21} = \frac{[\cos(2\theta) + 1][\cos(2\theta) - 1][\cos(2\phi) - 1]^2}{4},$$

$$e_{22} = \frac{[\cos(2\theta) + 1]^2[\cos(2\phi) - 1][\cos(2\phi) + 1]}{4},$$

$$e_{23} = -\frac{[\cos(2\theta) + 1][\cos(2\phi) + 1]\sin(2\theta)\sin(2\phi)}{2},$$

$$e_{31} = -\frac{[\cos(2\theta) - 1][\cos(2\phi) - 1]\sin(2\theta)\sin(2\phi)}{2},$$

$$e_{32} = -\frac{[\cos(2\theta) + 1][\cos(2\phi) + 1]\sin(2\theta)\sin(2\phi)}{2},$$

$$e_{33} = \sin^2(2\theta)\sin^2(2\phi), \tag{B21}$$

$$f_{11} = \frac{[\cos(2\theta) - 1]^2[\cos(2\phi) + 1][\cos(2\phi) - 1]}{4},$$

$$f_{12} = \frac{[\cos(2\theta) - 1][\cos(2\theta) + 1][\cos(2\phi) - 1]^2}{4},$$

$$f_{13} = -\frac{[\cos(2\theta) - 1][\cos(2\phi) - 1]\sin(2\theta)\sin(2\phi)}{2},$$

$$f_{21} = \frac{[\cos(2\theta) + 1][\cos(2\theta) - 1][\cos(2\phi) + 1]^2}{4},$$

$$f_{22} = \frac{[\cos(2\theta) + 1]^2[\cos(2\phi) + 1][\cos(2\phi) - 1]}{4},$$

$$f_{23} = -\frac{[\cos(2\theta) + 1][\cos(2\phi) + 1]\sin(2\theta)\sin(2\phi)}{2},$$

$$f_{31} = -\frac{[\cos(2\theta) - 1][\cos(2\phi) + 1]\sin(2\theta)\sin(2\phi)}{2},$$

$$f_{32} = -\frac{[\cos(2\theta) + 1][\cos(2\phi) - 1]\sin(2\theta)\sin(2\phi)}{4},$$

$$f_{33} = \sin^2(2\theta)\sin^2(2\phi). \tag{B22}$$

The expressions for D_j, E_j, and F_j in Eqs. (40)–(42) are obtained from A_j in Eq. (B16) by making the replacement $a_{ij} \to d_{ij}$, $a_{ij} \to e_{ij}$, and $a_{ij} \to f_{ij}$, respectively.

[1] B. R. Mollow, Phys. Rev. **188**, 1969 (1969).

[2] H. J. Kimble, M. Dagenais, and L. Mandel, Phys. Rev. Lett. **39**, 691 (1977).

[3] J. T. Höffges, H. W. Baldauf, W. Lange, and H. Walther, J. Mod. Opt. **44**, 1999 (1997).

[4] T. D. Ladd, F. Jelezko, R. Laflamme, Y. Nakamura, C. Monroe, and J. L. O'Brien, Nature (London) **464**, 45 (2010).

[5] A. Zrenner, E. Beham, S. Stufler, F. Findeis, M. Bichler, and G. Abstreiter, Nature (London) **418**, 612 (2002).

[6] X. Li, Y. Wu, D. Steel, D. Gammon, T. H. Stievater, D. S. Katzer, D. Park, C. Piermarocchi, and L. J. Sham, Science **301**, 809 (2003).

[7] X. Xu, B. Sun, P. R. Berman, D. G. Steel, A. S. Bracker, D. Gammon, and L. J. Sham, Science **317**, 929 (2007).

[8] A. Muller, E. B. Flagg, P. Bianucci, X. Y. Wang, D. G. Deppe, W. Ma, J. Zhang, G. J. Salamo, M. Xiao, and C. K. Shih, Phys. Rev. Lett. **99**, 187402 (2007).

[9] X. Xu, B. Sun, E. D. Kim, K. Smirl, P. R. Berman, D. G. Steel, A. S. Bracker, D. Gammon, and L. J. Sham, Phys. Rev. Lett. **101**, 227401 (2008).

[10] X. Xu, B. Sun, P. Berman, D. G. Steel, D. Gammon, and L. Sham, Solid State Commun. **149**, 1479 (2009).

[11] T. W. Mossberg and M. Lewenstein, Phys. Rev. A **39**, 163 (1989).

[12] Y. Zhu, Q. Wu, A. Lezama, D. J. Gauthier, and T. W. Mossberg, Phys. Rev. A **41**, 6574 (1990).

[13] H. Freedhoff and Z. Chen, Phys. Rev. A **41**, 6013 (1990).

[14] Z. Ficek and H. S. Freedhoff, Phys. Rev. A **48**, 3092 (1993).

[15] M. Peiris, K. Konthasinghe, Y. Yu, Z. C. Niu, and A. Muller, Phys. Rev. B **89**, 155305 (2014).

[16] K. Konthasinghe, M. Peiris, and A. Muller, Phys. Rev. A **90**, 023810 (2014).

[17] D. F. Walls and P. Zoller, Phys. Rev. Lett. **47**, 709 (1981).

[18] Z. H. Lu, S. Bali, and J. E. Thomas, Phys. Rev. Lett. **81**, 3635 (1998).

[19] H. Grote, K. Danzmann, K. L. Dooley, R. Schnabel, J. Slutsky, and H. Vahlbruch, Phys. Rev. Lett. **110**, 181101 (2013).

[20] S. Takeda, T. Mizuta, M. Fuwa, H. Yonezawa, P. van Loock, and A. Furusawa, Phys. Rev. A **88**, 042327 (2013).

[21] U. L. Andersen, J. S. Neergaard-Nielsen, P. van Loock, and A. Furusawa, Nat. Phys. **11**, 713 (2015).

[22] P. Drummond and Z. Ficek, *Quantum Squeezing* (Springer, Berlin, 2004).

[23] S. L. Braunstein and P. van Loock, Rev. Mod. Phys. **77**, 513 (2005).

[24] M. Macovei and G.-x. Li, Phys. Rev. A **76**, 023818 (2007).

[25] W. Vogel, Phys. Rev. Lett. **67**, 2450 (1991).

[26] C. H. H. Schulte, J. Hansom, A. E. Jones, C. Matthiesen, C. Le Gall, and M. Atature, Nature (London) **525**, 222 (2015).

[27] D. Martín-Cano, H. R. Haakh, K. Murr, and M. Agio, Phys. Rev. Lett. **113**, 263605 (2014).

[28] D. Martín-Cano, H. R. Haakh, and M. Agio, J. Opt. **18**, 024010 (2016).

[29] W. Fang, Q.-l. Wu, S.-p. Wu, and G.-x. Li, Phys. Rev. A **93**, 053831 (2016).

[30] V. A. Kovarskii, Phys. Usp. **42**, 797 (1999).

[31] P. W. Fry, I. E. Itskevich, D. J. Mowbray, M. S. Skolnick, J. J. Finley, J. A. Barker, E. P. O'Reilly, L. R. Wilson, I. A. Larkin, P. A. Maksym, M. Hopkinson, M. Al-Khafaji, J. P. R. David, A. G. Cullis, G. Hill, and J. C. Clark, Phys. Rev. Lett. **84**, 733 (2000).

[32] A. Patanè, A. Levin, A. Polimeni, F. Schindler, P. C. Main, L. Eaves, and M. Henini, Appl. Phys. Lett. **77**, 2979 (2000).

[33] R. J. Warburton, C. Schulhauser, D. Haft, C. Schäflein, K. Karrai, J. M. Garcia, W. Schoenfeld, and P. M. Petroff, Phys. Rev. B **65**, 113303 (2002).

[34] L.-s. Li and A. P. Alivisatos, Phys. Rev. Lett. **90**, 097402 (2003).

[35] C. Schulhauser, D. Haft, C. Schäflein, K. Karrai, R. J. Warburton, J. M. Garcia, W. Schoenfeld, and P. M. Petroff, Physica E **13**, 161 (2002).

[36] I. A. Ostapenko, G. Hönig, C. Kindel, S. Rodt, A. Strittmatter, A. Hoffmann, and D. Bimberg, Appl. Phys. Lett. **97**, 063103 (2010).

[37] M. Sugisaki, H.-W. Ren, S. V. Nair, K. Nishi, and Y. Masumoto, Phys. Rev. B **66**, 235309 (2002).

[38] R. Bavli and Y. B. Band, Phys. Rev. A **43**, 507 (1991).

[39] M. A. Antón and I. Gonzalo, J. Opt. Soc. Am. B **8**, 1035 (1991).

[40] V. P. Gavrilenko and E. Oks, J. Phys. B: At., Mol., Opt. Phys. **28**, 1433 (1995).

[41] A. Brown, W. J. Meath, and P. Tran, Phys. Rev. A **65**, 063401 (2002).

[42] G. N. Gibson, Phys. Rev. Lett. **89**, 263001 (2002).

[43] H. K. Avetissian, A. Brown, and G. F. Mkrtchian, Phys. Rev. A **80**, 033413 (2009).

[44] E. Paspalakis, J. Boviatsis, and S. Baskoutas, J. Appl. Phys. **114**, 153107 (2013).

[45] O. G. Calderon, R. Gutierrez-Castrejon, and J. M. Guerra, IEEE J. Quantum Electron. **35**, 47 (1999).

[46] F. Oster, C. H. Keitel, and M. Macovei, Phys. Rev. A **85**, 063814 (2012).

[47] O. V. Kibis, G. Y. Slepyan, S. A. Maksimenko, and A. Hoffmann, Phys. Rev. Lett. **102**, 023601 (2009).

[48] K. V. Kavokin, M. A. Kaliteevski, R. A. Abram, A. V. Kavokin, S. Sharkova, and I. A. Shelykh, Appl. Phys. Lett. **97**, 201111 (2010).

[49] I. G. Savenko, O. V. Kibis, and I. A. Shelykh, Phys. Rev. A **85**, 053818 (2012).

[50] G. G. Fedoruk, Phys. Solidi Status **46**, 1631 (2004).

[51] A. P. Saiko and G. G. Fedoruk, JETP Lett. **87**, 128 (2008).

[52] A. Papageorge, A. Majumdar, E. D. Kim, and J. Vučković, New J. Phys. **14**, 013028 (2012).

[53] A. Ulhaq, S. Weiler, C. Roy, S. M. Ulrich, M. Jetter, S. Hughes, and P. Michler, Opt. Express **21**, 4382 (2013).

[54] S. N. Shevchenko, A. N. Omelyanchouk, and E. Il'ichev, Low Temp. Phys. **38**, 283 (2012).

[55] G. Y. Kryuchkyan, V. Shahnazaryan, O. V. Kibis, and I. A. Shelykh, Phys. Rev. A **95**, 013834 (2017).

[56] Y. Yan, Z. Lü, H. Zheng, and Y. Zhao, Phys. Rev. A **93**, 033812 (2016).

[57] M. Macovei, M. Mishra, and C. H. Keitel, Phys. Rev. A **92**, 013846 (2015).

[58] V. B. Berestetskii, E. M. Lifshitz, and L. P. Pitaevskii, *Quantum Electrodynamics* (Butterworth-Heinemann, Oxford, 1996).

[59] S. Ashhab, J. R. Johansson, A. M. Zagoskin, and F. Nori, Phys. Rev. A **75**, 063414 (2007).

[60] A. Fashina and T. Nyokong, J. Lumin. **167**, 71 (2015).

[61] M. J. Frisch *et al.*, *Gaussian 09* (Gaussian, Inc., Wallingford, CT, 2009), Revision A.02.

[62] D. F. Walls and G. J. Milburn, *Quantum Optics* (Springer, Berlin, 1994).

[63] M. O. Scully and M. S. Zubairy, *Quantum Optics* (Cambridge University Press, Cambridge, UK, 1997).

[64] L. M. Narducci, M. O. Scully, G.-L. Oppo, P. Ru, and J. R. Tredicce, Phys. Rev. A **42**, 1630 (1990).

[65] M. Collett, D. Walls, and P. Zoller, Opt. Commun. **52**, 145 (1984).

[66] L. Childress and J. McIntyre, Phys. Rev. A **82**, 033839 (2010).

[67] A. P. Saiko and R. Fedaruk, JETP Lett. **91**, 681 (2010).

[68] S. Rohr, E. Dupont-Ferrier, B. Pigeau, P. Verlot, V. Jacques, and O. Arcizet, Phys. Rev. Lett. **112**, 010502 (2014).

[69] S. N. Shevchenko, G. Oelsner, Y. S. Greenberg, P. Macha, D. S. Karpov, M. Grajcar, U. Hübner, A. N. Omelyanchouk, and E. Il'ichev, Phys. Rev. B **89**, 184504 (2014).